IEEE Access
Multidisciplinary ⋮ Rapid Review ⋮ Open Access Journal

Received 28 February 2023, accepted 16 March 2023, date of publication 21 March 2023, date of current version 28 March 2023.

Digital Object Identifier 10.1109/ACCESS.2023.3260073

TOPICAL REVIEW

Electrical Reconfigurability in Modern 4G, 4G/5G and 5G Antennas: A Critical Review of Polarization and Frequency Reconfigurable Designs

RAZAN ALHAMAD, (Student Member, IEEE), EQAB ALMAJALI, (Member, IEEE), AND SOLIMAN MAHMOUD, (Senior Member, IEEE)
Electrical Engineering Department, University of Sharjah, Sharjah, United Arab Emirates
Corresponding author: Eqab Almajali (ealmajali@sharjah.ac.ae)

ABSTRACT This paper presents a critical review of modern 4G, 4G/5G, and 5G antennas, which employ PIN diodes and Varactors for polarization or frequency reconfiguration. For the reviewed 4G and 5G polarization reconfigurable antennas, a new parameter named spectrum utilization "AR/S_{11} B.W." is defined for the first time to predict the shared spectrum between the impedance bandwidth and the axial ratio bandwidth for circularly polarized antennas. The calculated spectrum utilization for many designs revealed that the majority of implementations failed to achieve full utilization of the available bandwidth. Besides, employing multiple PIN diodes is shown useful in improving the spectrum utilization and in supporting multiple polarization states. For the reviewed 4G, 4G/5G and 5G frequency reconfigurable antennas, the focus is mainly on comparing the available tuning range, fractional bandwidth and the Fractional Bandwidth Change (FBWC) upon tuning. The latter parameter, is defined and calculated in this work to measure the change in the FBW upon tuning. Utilizing multiple Varactors is shown promising in improving a 4G antenna's fractional bandwidth, while combining Multiple PINs and Varactors in one design is found efficient in improving the FBWC and the tuning range in the 5G spectrum.

INDEX TERMS Frequency reconfigurability, polarization reconfigurability, axial ratio bandwidth (AR B.W.), tuning range (TR), fractional bandwdith change (FBWC), PIN diodes, varactors.

I. INTRODUCTION

Wireless communication systems have been rapidly growing over the recent years. The new wireless technology, like the emerge of 4G and 5G communication systems, has set modern requirements to facilitate the user's experience such as enhanced bit rate, multi-standard applications and the electrical infrastructure to support it [1]. From a designer's point of view, a demand for creative antenna designs has unfolded to enable diverse communication schemes and bands with minimum cost [2]. These creative antennas need to be of a small footprint while covering several frequency bands (services) and can offer efficient bandwidth utilization as well as can communicate with diversely polarized antennas at once. This generally can not be electrically realized without reconfiguring an antenna design parameters. Antennas reconfigurability can refer to the ability to modulate and adjust the characteristics of an antenna such as its polarization, operating frequency and radiation pattern [3]. Antennas reconfigurability can be achieved by altering an antenna's electrical size and/or shape to control its operational characteristics such as frequency bands, polarization sense and radiation pattern. Frequency reconfiguration is crucial for a multi-standard supporting antenna, it overcomes the need of utilizing multiple antennas that resonate at different frequencies to transmit or receive a signal, which is area and cost efficient [4], [5], [6], [7].

The associate editor coordinating the review of this manuscript and approving it for publication was Hassan Tariq Chattha.

An antenna polarization can also be reconfigured to allow for frequency reuse and mitigation of multipath effects [8], [9]. An antenna's polarization usually depends on its physical layout as the direction of the surface current on its radiating parts is directly affected by the antenna shape and how it is excited. A reconfigurable polarization can capitalize an antenna's ability to change the polarization sense into different types (i.e., Linear (LP) to Circular (CP), Right -Hand Circular (RHCP) to Left Hand Circular (LHCP), etc.). This improves the ability to send and receive information from a greater number of diversely polarized antennas [10].

Implementing the aforementioned types of reconfigurability using electronic switches like PIN and Varactor diodes is one of the most commonly used techniques, which referred to as ''electrical reconfigurability'' [3], [11]. Due to the appealing features of electrical reconfigurability, like the low cost and the ease of implementation, it has attracted the attention of researchers over the past years. PINs and Varactors can be utilized to reconfigure single or multiple antenna parameters and can enable reconfgiruation at RF frequencies [3], [4], [5], [6], [7], [11], [12], [13], [14], [15], [16], [17], [18], [19], [20], [21], [22], [23], [24], [25], [26]. Other reconfiguration techniques have also been used to reconfigure antennas [27], [28], [29], [30], [31], [32], [33], [34], [35]. Table 1 highlights the advantages and disadvantages of different antennas reconfigurability methods reported in the open literature. Optical reconfiguration utilizes photo-conductive switches, formed by laser light incident on some semiconductor material [27]. Embedding this type of switches eliminates the need for metallic connections and biasing while providing fast switching speed [27], however, high optical power level is consumed through the laser light activation, especially in highly resistive Si [28]. Physically / Mechanically reconfigurable antennas is implemented by manually altering the structure of an antenna to enable reconfigurability [30], [31]. This technique does not utilize switches, rather than it implements motor, actuators and other mechanical ways to shift parts of the structure or change its electrical properties [32]. A common example would be a motor - based steerable reflectarry, such as the ones used in radars [36]. This mechanism is associated with low cost [31] but the implementation of actuators and other tools requires the use of high voltage and causes slow switching speed while occupying a large area [32], [37], [38]. Smart antennas is a fairly new mechanism that implements the reconfigurability using smart materials such as liquid metals [33], water [34] and oil [35]. The characteristics of an antenna can be controlled by pumping a fluid into a hollow behind the design to alter the substrate's characteristics such as magnetic permeability and electric permittivity [39], [40]. While it allows for a high power handling [40], this type of reconfigurability has limited applications due to the high cost of the materials used [41], such as Galinstan [35], while some other materials such as Mercury are known to be severely toxic [35].

TABLE 1. Basic comparison of the reconfigurability methods available in the open literature.

Technique	Merit/Demerit		Ref.
Optical Reconfiguration	Merit	Fast switching speed Eliminates biasing and wires	[27], [29]
	Demerit	High optical power required for activation Resistive semiconductor material	[28]
Physical/ Mechanical Reconfiguration	Merit	Low cost No external biasing and power requirements	[31], [32]
	Demerit	Low switching speed High voltage requirements Larger size to adapt actuator power supply	[32], [36]–[38]
Smart Antennas	Merit	Higher power handling Light weight	[39], [40]
	Demerit	Restrained applications Higher cost Toxic materials	[35], [41]
Electrical Reconfiguration	**Merit**	**Low cost Easier implementation Allows for multi - parameter reconfigurability Compact**	[18]–[26]
	Demerit	**Requires biasing**	

As this work deals with 4G and 5G antennas it is important to explore the bands and services licensed in the 4G and 5G spectrum. The fourth generation of cellular communication (4G) have been in action since introduced in a Circular Letter in 2008 [42]. Its allocated bands 0.45 GHz, 0.6 GHz, 0.7 GHz, 1.5 - 1.9 GHz, 2.1 - 2.6 GHz [43] are used for several applications including LTE 2300 (2.3 - 2.4), LTE 2500 (2.5 - 2.69), IMT - 2000 (1.92 - 1.98, 2.11 - 2.17), Bluetooth and WLAN (2.40 - 2.48) and GPS (1.559 - 1.61). This technology have been applied diversely including mobile multimedia [44], m-health [45], smart grids [46] and mobile internet access [47]. With the rising demand for higher data rate than the one offered by the 4G system, the fifth generation of cellular communication (5G) standard has been introduced. It offers great potential in terms of higher data rate [48], low latency and reliability [49]. Regulation authorities have generally classified 5G spectrum into low bands (Sub - 6 GHz) and high bands known as mm-wave spectrum [50]. The sub - 6 GHz spectrum is congested with both 4G and 5G applications [51],where ITU identified frequency bands include (0.47-0.698 GHz), (0.698 - 0.96 GHz), (1.427 - 1.518 GHz), (1.71 - 2.025 GHz), (2.11 - 2.2 GHz), (2.3 - 2.4 GHz), (2.5 - 2.69 GHz), (3.3 - 3.4 GHz), (3.6 - 3.7 GHz), (3.7 - 4.2 GHz), (4.4 - 4.99 GHz) [52], [53]. Licensed mm-wave bands include (24.35 - 27.5 GHz), (27.5 - 29.5 GHz), (37 - 40 GHz) and (60 - 71 GHz) [54]. 5G spectrum can facilitate diverse services such as enhanced Mobile Broadband (eMBB), which can be utilized for Augmented Reality (AR), cloud computing, 3D video and cloud storage [55], as well as enabling massive Machine Type Communications (mMTC) which can open the door for smart homes and smart cities development [52], [55], [56]. Since the sub - 6 GHz is crowded, 5G mm-wave frequency bands have been nominated for upcoming applications. However, the utilization of mm-wave devices have introduced challenges

including higher path loss when compared to sub - 6 GHz bands [57].

The objective of this paper is to critically review the recent state of the art works in the 4G, 4G/5G and 5G antennas, which utilize PIN and Varactor diodes to reconfigure the polarization and operating frequency, based on existing and newly defined and calculated figures of merits. The new figures of merit, namely, the spectrum utilization for polarization reconfigurability and the fractional bandwidth change (FBWC) for frequency reconfigurability are crucial in reviewing the bandwidth performance of modern reported works as they examine the effect of an antenna reconfiguration on the available bandwidth. The paper also provides a theoretical overview on how PIN and Varactor diodes are used to reconfigure an antenna's polarization state and operating frequency.

This review paper is organized as follows: Section II provides an overview on PIN and varactor diodes operating mechanisms and how they are used to reconfigure an antenna's polarization or operating frequency. Section III demonstrates a review and a comparison of state of the art polarization reconfigurable implementations for the modern 4G and the 5G applications. Section IV, includes a technical review with critical comparison of many sate of the art frequency reconfigurable works that cover services in the 4G, integrated 4G/5G and 5G spectrum. Section V presents important observations concluded from the critical review as well as it elaborates on related challenges and discusses future opportunities.

II. OVERVIEW ON THE USE OF PIN AND VARACTOR DIODES TO RECONFIGURE ANTENNAS

A. VARACTORS

A Varactor diode, also called as a Variable Capacitor, is an electronic device that is structured from a normal PN junction which behaves as a variable capacitor under varying reverse bias voltages [58]. The structure of varactors is built from an N type material and a P type material layered together. The width of the depletion region of a varactor grows with the square root of the reverse voltage applied in a nonlinear fashion, which decreases the junction's capacitance. This allows it to be used for tuning applications [6], [7], [59], [60]. To visualize the employment of a Varactor diode in tuning ''reconfiguring'' the frequency of an antenna, the configuration shown in Fig. 1 is considered. The structure was first reported in [61]. However, the parameters of the structure are altered here and the antenna is redesigned for enhanced performance. The new design parameters are listed in Table 2. The outline of the antenna shown in Fig. 1 includes two patches, one fed through an SMA connector, which is called ''main antenna'', while a second one ''tuning patch'' was added to tune the main antenna's resonant frequency via a Varactor diode integrated between the two. A Rogers Duroid 5880 is utilized as a substrate material with $\epsilon = 2.2$ and thickness of $h_s = 1.575$ mm. A SMV2019-040LF varactor model was considered, with a capacitance range of [0.23, 1.43] pF, capacitance ratio of [$C_{max}/C_{min} = 2.1$] and Q factor of 500 [62], [63].

TABLE 2. Frequency reconfigurable antenna design parameters.

Parameter	Value (mm)
L_{p1}	18.5
L_{p2}	15
L_v	1.05
W_p	30
H_s	1.575

The equivalent circuits of the varactor and the mictrsostrip patch are shown in Fig.1(b) and Fig.1(c), respectively, where the microstrip patch is modeled by a parallel RLC circuit [64], [65] and this is applicable to both the main and the tuning patches. The equivalent circuits demonstrate that the variable reactance offered by the varactor between the driven patch and tuning patch will affect the antenna's overall capacitive reactance (X_C) hence, it will tune its resonant frequency, given that other parameters in the varactor equivalent circuit have low values (the series resistance $R_s = 4.8\Omega$, the parasitic inductance due to packaging $L_s = 0.45\ nH$ and parasitic capacitance $C_p = 0.07\ pF$) [63]. The varactor's capacitance is characterized as $C_{var} = \epsilon A/d$, where it is a function of the dielectric constant ''ϵ'', junction area ''A'' and depletion region thickness ''d'' controlled by the reverse voltage applied. For the configuration shown in Fig.1, when the reverse bias voltage is increased, which in turns increases the junction's thickness ''d'', the Varactor capacitance (C_{var}), illustrated in Fig.1, will be decreased and the opposite happens when the bias voltage is decreased. Consequently, this will allow for frequency shift (tuning) as C_{var} will be added to the capacitance of the equivalent RLC circuit of the antenna, which is governed by $f_r = 1/2\pi\sqrt{L(C + C_{var})}$. The predicted reflection coefficient (S_{11}) results shown in Fig. 2, which is extraced from the CST model of the antenna shown in Fig.1 over the entire capacitance range supported by the Varactor model, tie very well with the resonant f_r relation mentioned earlier. It is evident that as C_{var} increases over the entire varactor span from 0.23 pF to 1.43 pF, the resonant frequency f_r is successfully reconfigured (tuned) down from almost f_r = 4.6 GHz to f_r = 2.9 GHz. The inverse proportionality between C_{var} and f_r allows frequency control according to $f_r = 1/2\pi\sqrt{L(C + C_{var})}$. As shown from Fig.2, a tuning range of 40.67 % (from 2.88 to 4.58 GHz) was scored with a minimum S_{11} matching of -17.8 dB. This indeed can be considered an incredible increment when compared to the original work [61] as the tuning range was limited to 27 %.

B. PIN DIODES

A PIN diode is a semiconductor element which functions as a variable resistor at RF and microwave frequencies under forward biasing conditions [66]. It is constructed from a P-type material and an N-type material with an intrinsic semiconductor I-region in between [67]. The I-region material affects the performance of the diode as it increases its

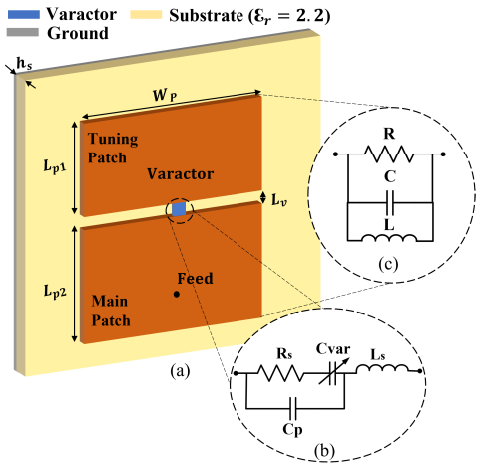

FIGURE 1. (a) Proposed illustrative structure on the frequency reconfigurability of an antenna using a Varactor. (b) equivalent circuit of the Varactor diode [63], (c) equivalent circuit of a microstrip patch [64], [65].

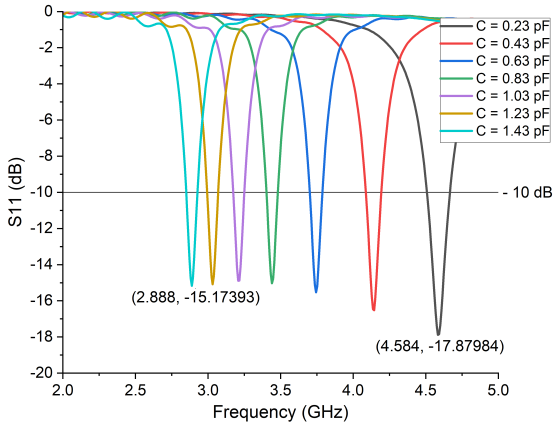

FIGURE 2. Frequency tuning upon varactor's capacitance change.

breakdown voltage [68]. To turn ON the diode, a forward bias voltage is applied. The depletion region will then immediately collapse and the carriers (holes / electrons) will be consequently injected to the intrinsic region. However, they do not combine immediately. Instead, a finite lifetime (τ) will be consumed till they combine in the I-region. While in forward bias, the I-region stores charges. Therefore, to turn OFF the diode, reverse bias voltage is applied but a time delay, called Reverse Recovery Time, occurs to eliminate those pent up charges [69]. PIN diodes can be operated as very efficient switches at RF frequencies, due to their ability to control the insertion loss using the series resistance's dependence on current [70]. This allows the diode to appear as either a low impedance with minimum insertion loss (ON state), or large impedance causing most of the energy to be reflected back (Off state).

To conceptualize on how these switches are utilized to reconfigure antennas, an example on the use of PIN diodes to reconfigure the polarization of an antenna is shown in Fig.3. The model shown was first reported in [71]. However, the design parameters were modified, and hence the antenna

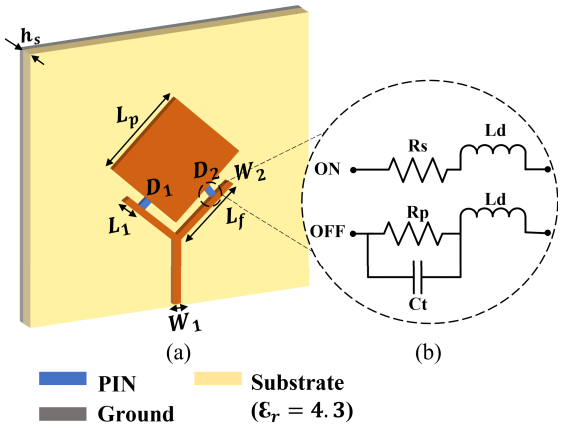

FIGURE 3. (a) Proposed illustrative structure on the polarization reconfigurability of an antenna using PINs (b) Equivalent circuit model of a PIN diode.

was redesigned, to elevate the operation from 4G in [71] to Sub-6 GHz (5G). The structure consists of a rhombus shaped patch antenna, fed by a Y-shaped feedline through two PIN diodes [72], built on FR-4 substrate with $\epsilon_r = 4.3$ and substrate thickness of $h_s = 1.4$ *mm*. The outline provides RHCP and LHCP diversity, depending on the states of the implemented PIN diodes, which are D1 and D2 shown in Fig.3). The geometry was simulated using CST Microwave Studio [73] to radiate at a center frequency of 3.5 GHz. The dimensions of the antenna are given in Table. 3.

The equivalent circuit model of a PIN diode is illustrated in Fig.3 (b) for both ON and OFF states. When D1 is ON (D2 is OFF), the patch antenna and the left branch line of the Y-shaped feedline are electrically connected. This aids the antenna to produce an electrically asymmetrical structure and this excites two orthogonal modes (TM_{10} and TM_{01}) [71], which have an equal amplitude and a 90° phase difference. The excited TM_{10} and TM_{01} modes,, when D1 is ON and D2 is off, are shown in Fig.4 (e) and (f), respectively. The slots are added to these figures to show that the TM_{10} mode is electrically longer than TM_{01} along the y-axis (the current curls around the right slot), hence, the current rotates in the clockwise direction. Consequently, the antenna presents a LHCP state. Fig. 4 (a), (b), (c), and (d) exhibit the surface current distribution extracted from the CST antenna model at 3.5 GHz, when D1 is ON and D2 is off, for four samples of the current at different phase values to illustrate the progressive current rotation with reference to the positive y-axis. This curling current in the clockwise direction produces an electric field that follows same behavior leading to the generation of LHCP wave. Similarly, when D2 is ON (D1 is OFF), the antenna provides a counterclockwise current rotation, therefore generating a RHCP state.

During the design process, the patch length L_p was tuned to be very close to $\lambda_{eff}/2$. One key parameter was investigated is the location of the PIN diode determined by L_1, which is responsible for the feeding location. While L_1 is important to obtain good matching, it was found important

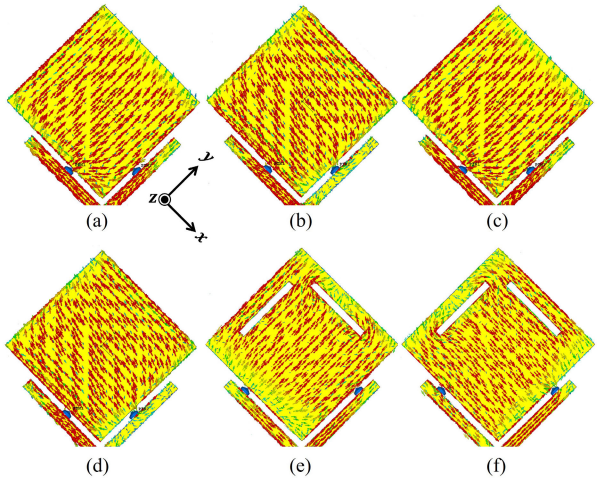

FIGURE 4. Surface current distribution predicted on the proposed antenna structure characterizing the LHCP state generation (a) 0° (b) 90° (c) 180° (d) 270° (e) TM_{10} mode (f) TM_{01} mode.

in determining the Axial Ratio (AR), which characterizes the circular polarization (CP) purity. An acceptable CP wave should always have an AR below 3dB. This is controlled mostly by determining the exact feeding location that outputs a circular polarization response. For further investigation, the axial ratio response was predicted at different L_1 values as illustrated in Fig.5. The best axial ratio was scored at $L_1 = 2.5$ mm, which results in a 1.43% 3-dB bandwidth. A minimum AR of 0.051 dB was predicted for the LHCP state. The PIN diode was modeled in CST using its equivalent lumped elements for the ON and OFF states. The element value and location can be defined in the Network Lumped Element listed under the Simulation tab. For the ON state, a series resistance of 1.5Ω, which represents the internal losses of the used PIN diode under forward biasing condition as reported in the data sheet of the PIN diode model HSMP-3860 in [72], is considered while the packaging L_d shown in Fig.3 is neglected as no packaging is considered. For the OFF state, the equivalent circuit of a PIN diode is shown in Fig.3 as an inductance L_d in series with a parallel RC circuit. R_p usually has a very large value to represent an open circuit and C_t is the depletion region's capacitance. Under reverse biasing conditions, the PIN diode depletion capacitance (C_t) is commonly dependent on the reverse voltage applied, due to the variation of the depletion region's width. However, if the intrinsic region is sufficiently wide, the depletion's capacitance is almost constant over a wide reverse voltage range. For the PIN diode model HSMP-3860, C_t value at a reverse bias voltage of 1V, which we considered in the simulation (0V to -1V), approximately equals 0.2 pF at 3.5 GHz as extracted from the data reported in [72], hence it was selected to model the PIN diode in the OFF state.

In addition to polarization diversity, PIN diodes are also used for frequency and pattern reconfigurability. For frequency reconfigurability, PIN diodes can be used as a bridge to connect/ disconnect metallic radiators to each other which

TABLE 3. Polarization reconfigurable antenna design parameters.

Parameter	Value (mm)
L_p	19
L_f	13
L_1	2.5
W_1	2.74
W_2	1.37
H_s	1.4

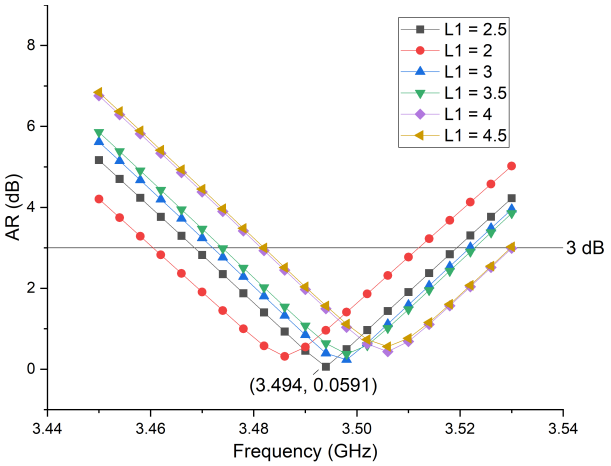

FIGURE 5. Axial ratio response for diverse feeding locations calculated at center frequency 3.5 GHz.

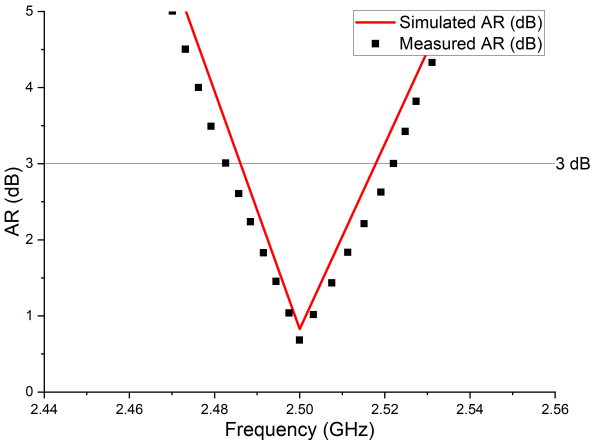

FIGURE 6. Simulated versus measured AR for the LHCP reported in [71].

can alter the effective length of the antenna, leading to frequency reconfiguration [15], [74], [75].

To compare the simulated AR results to measured ones, the polarization reconfigurability example reported in [71], which uses a PIN diode for polarization reconfigurability at 2.45 GHz, is simulated using CST for the AR of the LHCP. The simulated results are compared to the measured ones extracted from Fig. 8 (b) in [71]. As shown in Fig.6, the simulated AR values are in good agreement with the measured ones. This establishes the validity of the simulated results obtained using CST for the examples included in the paper.

III. POLARIZATION RECONFIGURABLE ANTENNAS

Polarization reconfigurability have been proposed in the early 1980s by Schaubert et al. [76]. The design proposed in [76] is a square patch fed from the corner with four pairs of microwave diodes which operate as switchable shorting posts located along the center lines to achieve slant polarization, Horizontal Polarization (HP),Vertical Polarization (VP), Right Hand Circular Polarization (RHCP) and Left Hand Circular Polarization (LHCP).

Since then, researchers have developed wide variety of similar designs or they have further enhanced the performance of this type of configuration to satisfy modern demands. Generally, two approaches are used to implement a polarization reconfigurable antenna by either using a reconfigurable radiator [77] or a reconfigurable feeding network [78], [79], [80], [81]. The latter is more desirable, and hence more utilized by researchers, as it is more convenient for achieving full polarization diversity, in which both Linear Polarization (LP) and Circular Polarization (CP) are implemented. This approach also results in a lower cross polarization level [82]. There are many diverse implementations of this type of reconfigurabiliy in both the 4G and the 5G spectrum [71], [77], [79], [80], [81], [82], [83], [84], [85], [86], [87]. Table 4 and Table 5 illustrate modern implementations of polarization reconfigurability in the 4G and 5G spectrum taking into account the main figures of merit related to polarization reconfigurbility. The Axial Ratio bandwidth (AR B.W.) in the tables symbolizes the spectrum over which the CP polarization is within the acceptable range for CP antennas (below 3 dB) [88], [89]. While the impedance bandwidth (S_{11} B.W.) is another important figure of merit for any antenna design, an antenna designer should carefully tune both the AR B.W. and the S_{11} B.W. with respect to the resonant frequency. Consequently, a considerable overlapping between AR B.W. and the S_{11} B.W. must be obtained to support the practicality (functionality) within the same spectrum. If an acceptable axial ratio bandwidth was obtained at frequencies with poor S_{11} matching, the design would not be of a practical value. This was not given enough consideration in many of the reported works in the literature, therefore, a new parameter is presented in this paper to calculate the percentage of overlapping between the AR B.W. and the S_{11} B.W. for all works included Table 4 and Table 5. This will allow for a real critical review for the state of the art. Fig.7 shows how the new parameter, which is called the spectrum utilization "AR/S_{11} B.W." and indicates the percentage of overlapping, is calculated. The AR/S_{11} B.W. therefore symbolizes the utilization of the accepted bandwidth for polarization reconfigurability. According to Fig.7, f_1 and f_2 mark the 10 dB impedance bandwidth (S_{11} B.W.) limits whereas f_a and f_b define the 3 dB limit for the AR (AR B.W.). For the work done in [86], which is included in Table 4, the S_{11} B.W. is 2.43 GHz - 2.72 GHz and the AR B.W. spans in 2.165 GHz - 2.67 GHz, therefore $\frac{AR}{S_{11}} = \frac{2.67-2.615}{2.72-2.43} \times (100) =$ 19%. This means only within 19% of the S_{11} B.W., the antenna is reconfigured for circular polarization. This shows the importance of this newly defined figure of merit in this paper as designs that achieve higher AR/S_{11} have better spectrum utilization. It is important to note that the calculation presented in Fig. 7 is valid as far as the AR B.W. is within the S_{11} B.W. or vice versa. Although the newly defined spectrum utilization (AR/S_{11} B.W.) figure of merit can be considered as an effective parameter to highlight the practically available bandwdith for the polarization reconfigurability for a given design, and hence how much that design can be improved, AR/S_{11} B.W. can also be used to compare between different designs, to measure the percentage of the obtained S_{11} B.W. than can be utilized for Circular Polarization as any remaining portion of the S_{11} B.W., that does not overlap with the AR B.W., will be useless as far as the polarization reconfigurability is concerned. Another figure of merit, that is listed in the tables is the number of achieved polarization states. This important parameter reflects the flexibility a design can offer to communicate with a broad number of antennas. Finally, the number of diodes employed is used as an indication for the complexity of the structure and listed as a figure of merit in Table 4 and Table 5, where designs employing three PIN diodes and more are commonly considered complex. Other design facets are taken into consideration as well when classifying the designs, such as the antenna's structure, biasing circuitry and number of layers, which highlight the design's complexity and cost.

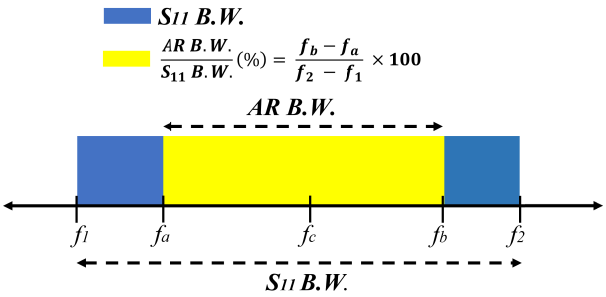

FIGURE 7. Illustration of the spectrum utilization (AR/S_{11} B.W.) calculation for CP antennas.

A. POLARIZATION RECONFIGURABILITY IN THE 4G SPECTRUM

Many authors have presented designs which utilize two PIN diodes to implement polarization reconfigurability in the 4G spectrum [71], [77], [79], [80], [82], [86], [87], [92], [94]. Khidre et al. [90] has proposed a simple design comprised of an E - shaped patch antenna printed on a single-layer substrate with a single feeding probe to excite the structure as shown in Fig.8. The antenna supports both Linear (LP) and Circular (CP) polarization states. As shown, two PIN diodes were inserted across the slots to control the polarization sense through changing the electrical length of the slots for a symmetrical or asymmetrical excitation. The design demonstrates an excellent AR/S_{11} B.W. of 100 % (spectrum utilization), which means a complete overlapping between

TABLE 4. Comparison of the state of the art 4G polarization reconfigurable antennas.

	Figures of Merits						
Ref.	**Antenna Structure**	**No. Switches**	**S_{11} B.W. (GHz)(%) (Fc (GHz))**	**Polarization States**	**AR B.W. (GHz)(%) (Min AR (dB))**	**AR/ S_{11} B.W. (%)**	**Application**
[86]	Square patch with a ring slot in the ground plane and a T-shaped feed (Simple)	2 PIN	LP: 2.53 – 2.61 (3.3%) CP: 2.43-2.72 (12.08 %) (2.4)	RHCP, LHCP, LP	2.615 - 2.67 (2.3%) (0.37 dB)	19%	WLAN WiFi Bluetooth
[71]	Rhombus shaped antenna with Y - feedline (Simple)	2 PIN	2.42–2.56 (5.62%) (2.5)	RHCP, LHCP	2.48–2.52 (1.6 %) (LHCP: 0.69 dB) (RHCP: 1.1 dB)	28.57%	WLAN WiFi Bluetooth
[90]	E-shaped patch fed through a coaxial cable (Simple)	2 PIN	2.4-2.575 (7%) (2.48)	RHCP, LHCP, LP	2.38-2.6 (8.8%) (0.5 dB)	100.00%	WLAN WiFi Bluetooth
[91]	Rectangular monopole with strips (Simple)	2 PIN	LP: 1.95 - 3.8 (63.8 %) (LP: 2.9) CP: 2 - 2.5 (20.8%) (CP: 2.4)	RHCP, LHCP, LP	2.33 - 2.44 (4.5 %) ($< 0.5dB$)	22.00%	WLAN WiFi Bluetooth
[92]	Patch antenna with circular slot (Simple)	2 PIN	LP: 2.3 - 2.78 (19.6%) RHCP: 2.21 - 2.69 (19.6%) LHCP: 2.13 - 2.68 (22.4%) (2.45)	RHCP, LHCP, LP	2.36 - 2.56 (8.1 %) (0.5 dB)	42.55%	WLAN WiFi Bluetooth
[93]	Square patch with ground loop slots (Simple)	2 PIN	CP: 2.37 - 2.43 (2.5%) LP: 2.385 - 2.415 (1.25 %) (2.4)	RHCP, LHCP, LP	2.39 - 2.41 (0.83%) (0.5 dB)	33.33%	WLAN WiFi Bluetooth
[87]	Annular slot antenna fed by a V-shaped coupling feedline (Simple)	2 PIN	RHCP: 2.31 - 2.62 (12.6 %) LHCP: 2.29 - 2.6 (12.6 %) LP: 2.3 - 2.83 (21.54 %) (2.46)	RHCP, LHCP, LP	2.4 - 2.5 (4.06 %) (0.75 dB)	34.48%	WLAN WiFi Bluetooth
[77]	Squared - shaped ring slot antenna with 4 stubs (Complex)	4 PIN	LHCP: 2.28 - 3.63 (45.7%) RHCP: 2.22 - 3.65 (48.7%) LP: 2.27 – 2.52 (10.4 %) (2.4)	RHCP, LHCP, LP	LHCP: 2.28 - 2.51 (9.58 %) RHCP: 2.3 - 2.5 (8.3%) (0.2 dB)	14.81%	LTE2300 WLAN
[80]	Patch antenna with cross feeding probes (Complex)	3 PIN	LP: 2.3 - 2.85 (21 %) CP: 2.2 - 2.6 (16.32 %) (2.45)	RHCP, LHCP, LP	19.2% (1.2 dB)	100.00%	WLAN WiFi Bluetooth
[82]	Stacked ring square antennas (Complex)	6 PIN	HP: 1.925 - 2.018 VP: 1.9 - 2.006 (5.35 %) CP: 1.94 - 2.01 (3.53%) (1.98)	RHCP, LHCP, VP, HP	LHCP: 1.94 - 2.009 (3.48 %) RHCP: 1.935 - 2.01 (3.78 %) (RHCP: 0.2 dB) (LHCP: 0.75)	100.00%	Military telemetry GPS Mobile phones (GSM)
[79]	Square patch fed by L-shaped probes (Complex)	8 PIN	1.2 - 1.65 (31.03 %) (1.45)	RHCP, LHCP	1.29 - 1.59 (20.8 %) (1.7 dB)	66.67%	GPS - L1
[94]	Four radiating arms with reconfigurable feeding network (Complex)	8 PIN	1.12 - 2.25 (61.08 %) (RHCP: 1.675) (LHCP: 1.85)	RHCP, LHCP	1.5 - 1.9 (23.5 %) (0.5 dB)	35.4%	GPS CNSS RFID
[95]	Square ring patch with dual feed (Complex)	2 Varactors	LP: 1.97 - 2.04 (3.48 %) CP: 2.035 - 2.13 (4.72 %) (2.01)	RHCP, LHCP, LP	1.4% ($< 0.5dB$)	29.60%	WLAN WiFi Bluetooth

AR B.W. and S_{11} B.W., with a fractional impedance and AR B.W. of 7% and 8.8%, respectively. The utilization of a single layer fabrication, as well as the use of small number of diodes, made the design simple while rendering very competitive performance.

The works reported in [71], [86], [87], [90], [91], [92], and [93] also utilized simple designs with two PIN diodes to achieve polarization diversity. All mentioned works were designed to serve applications in the 4G spectrum within the 2.4 GHz bands including WLAN, WiFi and Bluetooth. The design proposed in [71] offers only two polarization states, RHCP and LHCP, in contrast to the remaining mentioned designs which offer an additional LP state as well. Among these simple designs, the works in [90] and [92] offer the highest AR B.W. of 8.8 % and 8.1%, respectively. When taking the works done in [71], [86], [87], [91], and [93] into consideration, an important notion is highlighted on the use of simple structures with small number of PINs for polarization reconfigurability in the 4G spectrum, a very limited and impractical AR B.W. is obtained. This is noted from [71], [86], [87], [91], and [93], where the AR B.W. achieved was 1.6%, 2.3%, 4.06%, 4.5% and 0.83%, respectively.

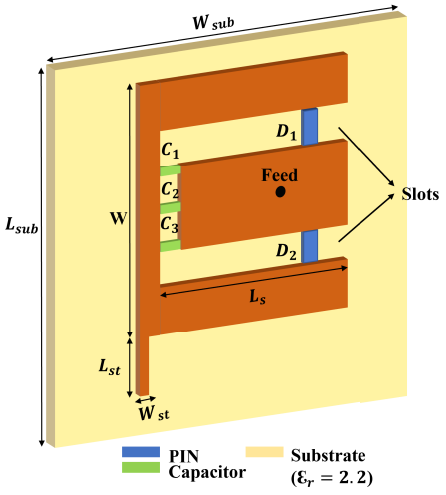

FIGURE 8. Polarization reconfigurability using a simple design with only two PIN diodes. Adapted from [90].

The calculated spectrum utilization (AR/S_{11} B.W) is listed for the designs in Table 4. When considering the works done in [71], [77], [86], and [91] where the calculated AR/S_{11} B.W. is 28.57%, 19%, 22% and 14.81%, respectively, it becomes clear that simple designs with small number of PINs offer humble spectrum utilization (AR/S_{11} B.W.) in the 4G spectrum. In this regard, the reported narrow $S_{11}B.W.$ in [71] and [93] produce reasonable spectrum utilization yet, the usable frequency band is very narrow. This underlines the question of what is required by the targeted application to say if these figures are satisfactory.

The polarization reconfigurability has been also implemented using diverse designs, which utilize more PIN diodes than the ones discussed thus far [77], [79], [80], [82], [94]. As described in Table 4, these appear to utilize more complicated antenna structures and more PIN diodes to realize the targeted polarization states. For instance, Wang and Wong [80] presented a patch antenna fed through a cross feeding probe at 2.45 GHz, as shown in Fig.9, offering CP and LP reconfiguration. The structure was built from three multi-layered substrates and four probes that support the cross feed built from three strips. Three PIN diodes were implemented between the strips to allow control over the polarization. When D1, shown in Fig.9 is ON, the current flows through Stub 1 and Stub 2, creating two orthogonal electric fields on the patch with a similar magnitude and 90° phase difference, resulting in a RHCP state. Similarly, when D2 is ON while D1 and D3 are OFF, the current flows through Stub 1 and Stub 3, leading to a LHCP state. For the LP state, D3 is ON while the rest are OFF, and the current is conveyed solely through Stub 1. This shows that the implementation of multiple PIN diodes offers a better control over the surface current, which facilitates reconfiguring multiple polarization states. The DC biasing circuit was embedded at the bottom substrate which was backed by the ground plane. The design achieved a 19.2 % AR B.W. and 16.32 % S_{11} B.W.. The AR/S_{11} B.W. is 100% which indicates the excellent spectrum utilization provided by the antenna. The outline of the antenna is characterized with multiple layers and PINs, which increase the overall cost and complexity.

Designs reported in [79] and [82], [94], which employ six and eight diodes, respectively, targeted a different frequency band of 1.559 - 1.61 GHz which serves applications including GPS and CNNs [96]. Both [79], [94] have offered only CP diversity, with AR/S_{11} B.W. of 66.67% and 35.4%, respectively, while [82] offered four polarization states with full spectrum utilization, where AR/S_{11} B.W. is 100%. Although Varactors are scarcely used for polarization reconfigurability, an antenna design based on two Varactors with figures of merits that are of interest was proposed in [95]. The structure resulted in a very narrow AR B.W. of only 1.4 % when compared to other works with similar layout and frequency of operation, in addition to the limited spectrum utilization, where AR/S_{11} is 29.6%.

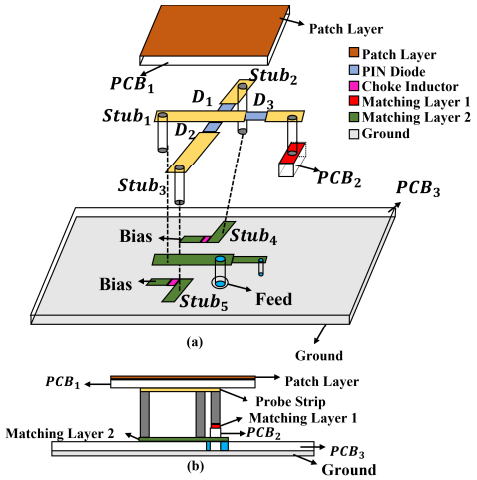

FIGURE 9. Polarization reconfigurability in the 4G spectrum using multiple PIN diods. Adapted from [80].

A key observation on polarization reconfigurability in the 4G spectrum:

- The utilization of multiple PINs improves the axial ratio (AR B.W.) bandwdith and the spectrum utilization (AR/S_{11}B.W.). This can be observed when comparing [79], [80], [82], [87] (100%, 66.67%, 100%, 34.48%, respectively) to [71], [77], [86], and [91] (28.57%, 19%, 22% and 14.81%, respectively) in Table 4 in terms of AR/S_{11} B.W. as well as when comparing [79], [80], [94] (19.2%, 20.8%, 23.5%, respectively) to [71], [86], [91] and [93] (1.6%, 2.3%, 4.5% and 0.83%, respectively) in terms of the achieved AR B.W.

B. POLARIZATION RECONFIGURABILITY IN THE 5G SPECTRUM

PIN and Varactor diodes were also used to employ polarization diversity in the 5G spectrum [78], [81], [84], [85], [97], [99], [100], [101]. Researchers have developed both simple designs with two diodes [97] and complex ones with multiple diodes [78], [84], [85], [98] as classified in Table 5. An advanced structure was demonstrated by Wu et al. in [98] as shown in Fig.10. The design consists of multiple layers. A 3×4 patch array is printed on the upper substrate, shown in Fig.10 (a), nine PIN diodes were used to electrically connect the patches, enabling polarization reconfgiruability based on the diodes states, while eight inductors are implemented to electrically connect the elements along the direction of polarization. The bottom substrate, shown in Fig.10 (b), was utilized for the DC biasing lines, as well as a co-planar waveguide (CPW). In between both substrates, a ground plane was implemented with a slant slot at $\theta = 40°$. The structure offers LP as well as LHCP senses depending on the PINs states. The antenna covers the 5G WiFi communications band with a high AR/S_{11} B.W. of 75 %. This is a very reasonable spectrum utilization as the AR B.W. and the S_{11} B.W. are reasonably wide; 16.36% and 21.8%, respectively.

TABLE 5. Comparison of the state of the art 5G polarization reconfigurable antennas.

	Figures of Merits						
Ref.	**Antenna Structure**	**No. Switches**	**S_{11} B.W. (GHz)(%) (Fc (GHz))**	**Polarization States**	**AR B.W. (GHz)(%) (Min AR (dB))**	**AR/ S_{11} B.W. (%)**	**Application**
[97]	Square patch with a semi ring slot (Simple)	2 PIN	LHCP: 3.25 - 3.6 (10.3 %) RHCP: 3 - 3.5 (14.7 %) (3.4)	RHCP, LHCP	3 - 3.7 (20.5 %) (2 dB)	100.00%	3.5 GHz WiMAX
[84]	Quadruple gap-coupled patches with L-shaped driven diploe (Complex)	4 PIN	4.61 - 4.97 (7.5 %) (4.8)	RHCP, LHCP, LP	4.6-4.95 (7.1 %) (2 dB)	94.44%	Radio Astronomy
[85]	Aperture coupled magnetoelectric dipole (Complex)	4 PIN	5.07 – 5.95 (16 %) (5.5)	RHCP, LHCP, LP	5.07-5.95 (16 %) (0.4 dB)	100%	5 GHz WiFi
[98]	3x4 array (Complex)	9 PIN	LP: 5.2 - 6.2 (18.18 %) RHCP: 5.2 - 6.4 (21.8 %) (5.5)	LP, LHCP	5.5 - 6.4 (16.36%) (1.5 dB)	75.00%	5 GHz WiFi
[78]	Circular patch with eight reconfigurable coupling loop stubs and wheel - shaped radiator (Complex)	64 PIN	CP: 3.45 - 4.6 (31.5 %) LP: (3.35 - 3.44), (4.5 - 4.75) (3.65)	RHCP, LHCP, LP	3.6 - 4.2 (16.4 %) (0.7 dB)	52.2%	3.5 GHz WiMAX
[99]	Patch fed through tunable quasi - limped coupler (Complex)	2 Varactors	3 - 3.72 (20.57%) (3.5)	RHCP, LHCP, VP, HP	3.433 - 3.567 (3.8%) (0.6 dB)	19%	3.5 GHz WIMAX
[100]	MIMO with reconfigurable feed (Complex)	4 PIN	26.13- 29.46 (11.9%) (28)	VP, HP	N/A	N/A	Satellite Communications
[101]	Square patch with 4 ground loop slots (Complex)	4 PIN	LP: 27.6 - 29.48 (6.7 %) CP: 27 - 29.07 (7.4 %) (28)	RHCP, LHCP, LP	1.50%	20.27%	Satellite Communications
[81]	2x2 tilted array (Complex)	4 PIN	26.5 – 29 (8.9 %) (28)	RHCP, LHCP	27.2 – 28.35 (4.1 %) (0.7 dB)	46.00%	Satellite Communications

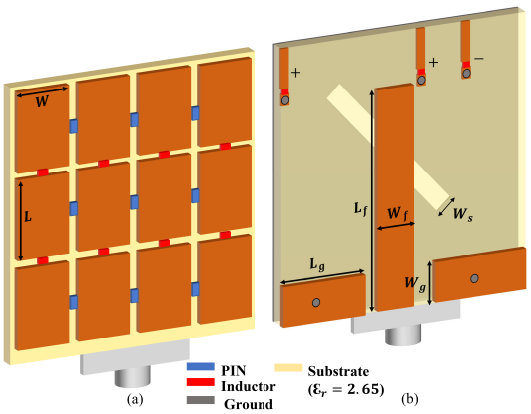

FIGURE 10. Polarization reconfigurability in the 5G spectrum using multiple PIN diodes. (a) front view and (b) back view. Adapted after [98].

The work done in [84] and [85] offer both LP and CP diversity reconfigured using four PIN diodes. The design in [85] was superior in terms of AR B.W. (16 %) as well as the spectrum utilization AR/S_{11} B.W. (100%), compared to the one in [84] which offers only 7.1% AR B.W. and 94.44 % AR/S_{11} B.W.. Despite the work done in [98] utilized nine PIN diodes, it achieved less polarization states (only LP and LHCP) with narrower AR/S_{11} B.W. (75%) compared to the design in [85] which supports the same frequency band and utilizes only 4 PIN diodes. On a similar observation, the work done in [78] used 64 diodes to achieve polarization diversity within the frequency range in [97], yet, the spectrum utilization in [78] (AR/S_{11} B.W. = 52.2 %) is almost half of it is in [97] (AR/S_{11} B.W. = 100%). It is observed that utilizing multiple PIN didoes does not ensure better performance for polarization diversity, as seen from comparing [85] and [98], as well as [78] and [97] in terms of AR/S_{11} B.W.

Despite Varactor diodes are not commonly used to reconfigure polarization in the 5G spectrum, the design in [99] utilized two Varactor diodes to offer four polarization states, with CP and LP diversity. The reported spectrum utilization AR/S_{11} B.W. in [99] is only 19%, which is humble as compared to the full spectrum utilization achieved in [97] of 100%. Reconfigurable polarization works were also reported for 5G mm - wave applications as proposed in [81], [100], and [101]. All proposed structures in are designed in the Ka band at a center frequency of 28 GHz for satellite communication purposes and all utilized four PINs to implement polarization diversity. The work done in [100] presented the widest S_{11} B.W. (26.13 - 29.49 GHz) while offering only LP diversity (VP and HP). On the other hand, the work done in [81] offered a much better spectrum utilization with AR/S_{11} B.W. of 46% compared to AR/S_{11} B.W. of 20.27% for the work in [101], however, the latter work has the advantage of offering LP state in addition to the two CP polarization states as shown in Table 5.

The key observations on polarization reconfigurability in the 5G spectrum are:

- Polarization diversity in the Sub-6 GHz 5G is mostly implemented using multiple PIN diodes. This stems from the fact that PIN diodes have a discrete nature (ON / OFF) which makes it easy to switch between polarization states when PINs are implemented in the feeding network of the antenna.
- Unlike 4G spectrum, utilizing multiple PINs does not ensure better AR B.W. and spectrum utilization (AR/S_{11} B.W.). However, utilizing multiple PINs can support multiple polarization states [78], [84], [85].
- Polarization reconfigurability in the mm - wave spectrum requires arrays and MIMOs for implementation while tuning can be achieved using small number of PINs [81], [100].
- PIN diodes are the chosen switching element for all works in the mm - wave 5G bands. This is a natural choice as Varactors own limited time response, which limits a varactor response from following the fast switching at mm-wave frequencies.

IV. FREQUENCY RECONFIGURABLE ANTENNAS

Modern wireless devices offer limited area for integrated antennas. This recent circumstance has increased the demand for tuning the 4G and 5G antennas to serve at multiple frequency bands. The idea of frequency reconfiguration to enable devices to switch between different communications frequency bands dynamically [14] is not new but there is a rising interest in it. Historically, frequency reuse was first used in satellite communications [102]. One of the first frequency reconfigured antenna designs, which utilized switches to implement reconfigurability, was published in the early 1980s by Schaubert et al. [76]. The proposed design was fairly simple. It comprised of a rectangular patch fed through a coaxial cable, with a pair of reconfigurable shorting posts along the center line, allowing for 20 % tuning range.

Many modern implementations have employed electronic elements such as PIN didoes and Varactors to reconfigure the frequency. Table 6, Table 7 and Table 8 illustrate state of the art 4G, integrated 4G/5G and 5G frequency reconfigured antennas mainly taken form the recent literature. The tables include chosen figure of merits. The antenna structures are classified into simple and complex, depending on the number of switches, layers and overall biasing circuitry required for a given design. Under this notion, designs with more than two PINs or Varactors are considered more complex. The center frequency as well as the 10 dB impedance bandwidth (S_{11} B.W.) are essential to highlight the applications and operational bandwidth of the design. The (S_{11} B.W.) is also called Fractional Bandwidth (FBW). The footprint of the design indicates the ability of integrating the concerned antennas into modern 4G or 5G devices. The Tuning Range (TR), which is not frequently reported by researchers, provides an indication on how wide the frequency range over which a design can be configured. This reflects the flexibility and capacity a design can offer. TR is calculated in all tables from the data reported in the concerned references as follows: $TR(\%) = 2(Fc_{max} - Fc_{min})/(Fc_{max} + Fc_{min}) \times (100)$. For example, the work done in [103], which is demonstrated in Table 7, presented frequency reconfigurability corresponding to three center frequencies 2.4 GHz, 3.5 GHz and 5.35 GHz with FBW of 8.7%, 11.2% and 11%, respectively. Therefore, the TR would be calculated as $TR(\%) = 2(5.35-2.4)/(5.35+2.4) \times (100) = 76.13\%$.

Under this context, a new figure of merit is proposed in this work, which is called "Fractional Bandwidth Change (FBWC)" as illustrated in Fig.11, to characterize the improvement or deterioration in the Fractional Bandwidth (FBW) across the tuning range. In this regard, the improvement or deterioration is determined according to the change in FBW as the frequency increases (tuning from f_1 to f_2 and then f_3 in Fig.11) because more bandwidth is needed to accommodate the modern demands of enhanced data rate and multi - services. By comparing the FBW offered at the lowest center frequency (f_1) of the reconfigurable band with the FBW offered at other center frequencies (f_2 and f_3), one can calculate the FBWC value, where a positive percentage value will indicate FBW improvement while a negative percentage indicates FBW reduction with respect to the FBW at the lowest centre frequency (f_1). As illustrated in Fig.11 and using the previous example, used for TR calculation, [103], the FBWC is calculated, with reference to Fig.11, as follows: $FBWC(\%) = \frac{11.2-8.7}{8.7} \times (100) = 28.73\%$ for the second band and $FBWC(\%) = \frac{11-8.7}{8.7} \times (100) = 26.43\%$ for the third band. This shows that the frequency reconfiguration in [103] achieved FBW improvements of 28.73 % and 26.43 % upon tuning the band from f_1 = 2.4 GHz to f_2 =3.5 GHz and f_3= 5.35 GHz, respectively.

It should be noted that while the above FBWC calculation is feasible with discrete bands offered by the employment of PIN diodes, designs employing varactors are more challenging due to the continuous tuning of the bands upon tuning. Therefore, the FBW will be represented as a range between the narrowest and largest FBW found in the respective work. If the narrow FBW corresponds to the lower center frequency, then the FBW is improving as the frequency increases upon tuning (the widest FBW is found at the higher center frequency), and vice versa. Therefore, to calculate the FBWC, the narrowest and the widest FBW are used, and by looking at their center frequencies, it can be determined whether its improving or deteriorating. As an example, the work done in [104] offered a TR across $F_c = 1.73 - 1.93$ GHz, where the FBW ranges from 2.3% to 4.59% from lower to higher frequencies. In this case, the FBWC is calculated as: $FBWC(\%) = \frac{4.59-2.3}{2.3} \times (100) = 99.56\%$. This is an excellent example on a decent improvement for the FBW upon tuning.

It is important to highlight that some figures of merit namely, TR, FBWC and footprint were calculated/estimated based on the data/figures provided in the respective

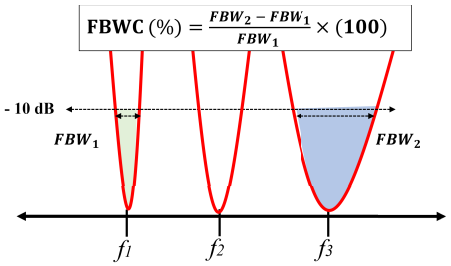

FIGURE 11. Fractional Bandwidth Change "FBWC" characterization and calculation.

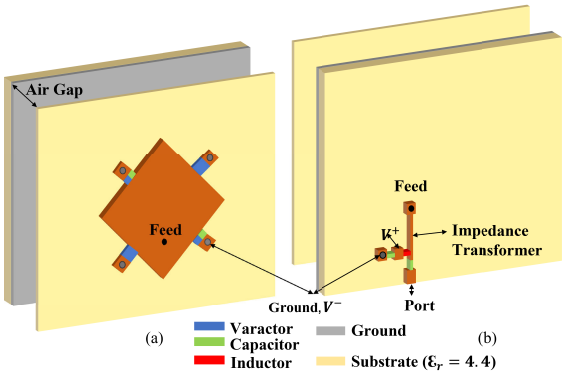

FIGURE 12. Frequency reconfigurable antenna design using multiple varactors. Adapted from [107].

references. The extracted measures used are namely, S_{11} B.W. and FBW. While the S_{11} B.W. can be clearly extracted in discrete tuning approaches, for continuous tuning approaches it is challenging to determine the exact S_{11} B.W. for each center frequency in the tuning range, therefore it is represented as the overlapped spectrum, where, under this notion, the FBW is represented as a range of available bandwidth when the antenna is tuned.

A. FREQUENCY RECONFIGURABILITY IN THE 4G SPECTRUM

Many recent works in the open literature have presented frequency reconfigurable 4G antennas using PINs and Varactors [7], [74], [104], [105], [106], [107], [108], as shown in Table 6. Row and Tsai [107] proposed a right hand circularly polarized square patch with 4 varactor diodes connected to the center of the four edges of the patch, as illustrated in Fig.12, to tune the frequency between (1.97 - 2.53 GHz) for WLAN applications. The design consists of multiple substrate layers separated by an air gap, where the top layer is used for the patch antenna and the bottom layer is used for the feedline and biasing circuits. The employed varactors are identical and are used to tune the resonant frequencies of the dual orthogonal modes (TM_{10}, TM_{01}) responsible for the RHCP, while the capacitors are utilized to produce the required phase difference of the two modes. The design accomplished a TR of 44.8 %, with a FBW ranging from 4% to 9.09%, leading to a significant improvement in the FBW, with a FBWC of 127.25%.

Varactors were used to implement frequency reconfigurability in the 4G spectrum with relatively more designs than the ones in which PINs are employed [7], [104], [106], [107], [108]. The proposed designs in [106], [107], and [108] have opted for similar frequency ranges around 2.4 GHz, using two, four and eight varactors, respectively. The designs support multiple services such as WLAN, Bluetooth and LTE. The designs in [106], [107], and [108] offered a FBW of 1.63%, 9.09% and 17.42%, respectively. A clear improvement can be noted between the number of Varactors employed and the resulting FBW, where the available FBW for WLAN and Bluetooth applications increases with number of Varactors used. This indicates better coverage for the applications at hand. The same trend can be noted in terms of the FBWC, where the works in [106], [107], and [108] achieved a FBWC of -58.25%, 127.25% and 190.33%, respectively. In terms of the TR, the antennas in [107] and [108] achieved a TR of 24.88% and 32.91%, respectively, which confirms the performance improvement as the number of varactors increases.

Furthermore, the works done in [7] and [104] are designed for GPS services using eight and twenty five varactors, respectively. The work in [7] have offered a significant advantage of providing independently reconfigurable dual bands centered around 0.9 GHz and 1.7 GHz, while [104] offer a single reconfigurable band centered around 1.8 GHz. The second band offered by [7] (1.5 - 1.87 GHz) greatly overlaps with that offered by [104] (1.72 - 1.95 GHz), however, the achieved FBW, TR as well as FBWC by utilizing 8 varactors in [7] (6%, 22% and 500%) are larger than the ones achieved using 25 varactors in [104] (4.59%, 13% and 99.56%).

On the other hand, PIN diodes are also used to tune bands in the 4G spectrum used for WLAN, GPS and GSM [74], [105]. As summarized in Table 6, the design proposed in [74] utilize a single PIN diode to tune dual bands centered around (1.55, 2.55 GHz) to (1.65, 2.49 GHz). While the dual band approach is advantageous, the FBW obtained in the first band is low (0.64%), and it is improved to 1.81% upon tuning. On the other hand, the FBW achieved in the second band has noticeably deteriorated upon tuning with FBWC of -41.6% (FBW = 2.55% to 1.6%). This indicates that the available FBW may not fully cover the 2.4 spectrum for WLAN services. When comparing [74] to [105], in which a single band is tuned into four bands across 1.6 - 2.71 GHz by employing three PINs, a larger FBW is obtained in each designated band in [105], ranging from 6% to 17%. This shows that the use of large number of PINs, increases the FBW and hence the FBWC for WLAN and WiFi services as confirmed from the figures reported in [74] and [105]. Finally, in terms of the services provided in the 4G spectrum, designs in [107] and [108] support most of the applications successfully, while [7], [104] can only support GPS. Furthermore, the design in [106] offers great solution for cognitive radio applications. However, the narrow FBW offered can partially satisfy WLAN and LTE applications whereas the design in [105] can satisfy services like LTE, Bluetooth and WLAN.

TABLE 6. Comparison of the state of the art 4G frequency reconfigurable antennas.

	Figures of Merits							
Ref.	**Antenna Structure**	**No. of Switches**	**Fc (GHz)**	**S_{11} B.W. (GHz)(FBW %)**	**TR (%)**	**FBWC (%)**	**Footprint (mm^2)**	**Application**
[74]	Multilayered patch antenna (Complex)	1 PIN	Dual bands: (1.55,2.55) (1.65 , 2.49)	(1.545 - 1.555) (0.64%) (2.515-2.585) (2.55%) (1.642-1.657) (1.81%) (2.47 - 2.51) (1.6%)	6.25%, 2.38%	(182.81%, -41.6%)	80.3 x 80.3	GPS WiFi WLAN
[105]	Four rectangular dielectric resonators antenna with slotted ground (Complex)	3 PIN	2.15	(1.6 - 1.91) (17%) (1.93 - 2.15) (11%) (2.24 - 2.57) (14%) (2.55 - 2.71) (6%)	36.36%	-35.3% -17.64% -64.70%	20 x 36	GSM LTE WLAN
[106]	Two elements MIMO antenna based on pentagonal slots in the ground (Simple)	2 Varactors	2.13	(1.64 - 2.62) (1.63% - 1.03%)	44.60%	-58.25%	60 x 120	Cognitive Radio WLAN Bluetooth
[107]	Square patch antenna (Complex)	4 Varactors	2.25	(1.97 - 2.53) (4% - 9.09%)	24.88%	127.25%	N/A	WLAN Bluetooth LTE 2300 LTE 2400
[108]	Stepped impedance dipole antenna (Complex)	8 Varactors	2.45	(1.98 - 2.76) (6 % - 17.42%)	32.91%	190.33%	60 x 30.6	WLAN Bluetooth LTE 2300 LTE 2400
[7]	Dual band slotted monopole antenna (Complex)	8 Varactors	Dual band: (0.9, 1.7)	(0.76 - 1.04) (1.9%) (1.5 - 1.87) (1% - 6%)	31%, 22%	(0%, 500%)	88 x 88	GPS
[104]	Planar active artificial magnetic conductor (AAMC) frequency reconfigurable antenna (Complex)	25 Varactors	1.8	(1.72 - 1.95) (2.3% - 4.59%)	13.00%	99.56%	125 x 125	GPS

The key observations on frequency reconfiguration in the 4G spectrum are:

- The employment of multiple Varactor diodes improves the fractional bandwdith (FBW), as well as the change in the fractional bandwidith (FBWC) for the Bluetooth and WLAN applications, as seen from the designs in [106], [107], and [108].
- Varactors entail a fractional bandwdith FBWs that steadily increase with frequency tuning [7], [107], [108]. Therefore, the FBWC values obtained using Varactors are higher than the ones achieved using PIN diodes in WLAN, Bluetooth and GPS bands.
- Varactors outperform PINs for frequency tuning due to their ability in covering most of the desired bands while offering distinct frequency selection in a continuous manner.

B. INTEGRATED 4G/5G FREQUENCY RECONFIGURABLE ANTENNAS

The idea behind frequency tuning have emerged from the need to support multiple standards in the 4G and 5G spectrum using the same hardware. Under this context, in several modern works multiple 4G and 5G (Sub-6 GHz) services were supported by one integrated 4G/5G antennas [4], [15], [19], [61], [103], [109], [110], [111], [112] as illustrated in Table 7.

Han et al. [109] proposed a patch antenna designed with two L -shaped and one U - shaped slots engraved in the ground as illustrated in Fig.13. Three PIN diodes are utilized for frequency reconfigurability in the 4G and the Sub-6 GHz 5G spectrum, to cover LTE 2300, AMT and WLAN services. Diode D1, shown in Fig.7, controls the band response, switching between dual bands when D1 is OFF and a single band when D1 is ON, while D2 and D3 are utilized to tune the operating frequency in each of the bands namely, (2.39, 4.59 GHz) when both D2 and D3 are OFF, and (4.32, 5.64 GHz) when both are ON. One highlight for this design is the excellent TR in the designated bands with a TR of 86.42 % and (57.5%, 20.5%) for the single and dual bands, respectively. In addition, the obtained FBW improves upon tuning to higher frequencies, as can be observed for both the single band (FBW = 2.6% to 6.5%) with an excellent FBWC of 150%, as well as the dual bands (FBW = 6.7% to 7.4%, 2.7% to 4.6%) with FBWC of 10.44% and 70.37%, respectively. The employment of multiple diodes makes the design relatively complex.

Other structures, which utilizes PIN diodes to tune frequency in the 4G/5G spectrum, are reported in [4], [15], and [109]. In these modern designs, the FBW provided was reconfigured between a single band and dual bands [4], [15], [109], as well as triple bands [4]. The works done in [15], [109], and [4] support multiple applications including 5G

TABLE 7. Comparison of the state of the art 4G and 5G frequency reconfigurable antennas.

	Figures of Merits							
Ref.	**Antenna Structure**	**No. of Switches**	**Fc (GHz)**	**S_{11} B.W. (GHz) (FBW %)**	**TR (%)**	**FBWC (%)**	**Footprint (mm^2)**	**Application**
[15]	Two asymmetrical L-shaped patches (Simple)	1 PIN	Single band: 4 Dual bands: (2.4 , 5.3) (3.3,5.9)	Single band: 3.6 - 4.8 (30%) Dual bands: (2.1 - 2.5)(16.66%) (5 - 5.6)(11.3%) (2.8 - 3.6)(24.24%) (5.5 - 6.1)(10.16%)	Dual bands: (31.57%,10.71%)	Dual bands: (45.5%, -10.08%)	40 x 35	2.4 GHz WLAN Bluetooth 5G WiFi
[109]	Patch antenna with U shaped and two symmetrical L-shaped slotted ground (Complex)	3 PIN	Single bands: (2.42 , 5.66) Dual bands: (2.39, 4.59) (4.32, 5.64)	Single band: (2.32 - 2.38)(2.6%) (5.49-5.86)(6.5%) Dual Bands: (2.28 - 2.44)(6.7%) (4.38 - 4.5)(2.7%) (4.16 - 4.48)(7.4%) (5.5 - 5.76) (4.6%)	Single band: 86.42 % Dual band: (57.5%, 20.5 %)	Single band: 150% Dual bands: (10.44%, 70.37%)	27 x 25	LTE 2300 AMT 5G WiFi 2.4 GHz WLAN
[103]	Microstrip square slot antenna (Complex)	3 PIN	2.4, 3.5, 5.35	(2.3 - 2.51)(8.7%) (3.35 - 3.75)(11.2%) (4.95 - 5.53) (11%)	76.13%	26.43% 28.73%	20 x 20	2.4 GHz WLAN Bluetooth 5G WiFi 3.5 GHz WiMAX
[4]	L - shaped monopole (Complex)	4 PIN	Single bands: (3.5, 5) Dual bands: (2.6, 6.5) (2.1, 5.6) Triple bands: (1.8, 4.8, 6.4)	Single bands: (3.03-4.42)(39.71%) (4.21-5.61)(28%) Dual bands: (2.4 - 2.9)(19.23%) (6.27-6.94)(10.3%) (1.95 - 2.25)(14.28%) (5.41-5.86)(8.03%) Triple bands: (1.71-1.9)(10.55%) (4.55-5.13)(12.08%) (6.18-6.63)(7.03%)	Single bands: 35.29% Dual bands: (21.27%, 14.88%)	Single bands: -29.48% Dual bands: (34.66%, 28.26%)	40 x 32	2.4 GHz WLAN Bluetooth 5G WiFi 3.5 GHz WiMAX GPS
[19]	Differentially fed antenna with a slotted circular patch (Complex)	4 PIN	2.45, 3.5	(2.37 - 2.67)(12.24%) (3.39 - 3.62) (6.57%)	27.28%	-46.32%	100 x 100	2.4 G WLAN Bluetooth WiMAX
[110]	Microstrip Patch-Slot Antenna (Complex)	5 PIN	3.59, 3.41, 3.24, 3.03, 2.47, 2.3, 2.19, 2.05, 1.98	(3.5-3.68)(5.1%) (3.31 - 3.5)(5.5%) (3.165-3.31)(4.6%) (2.95-3.1)(5%) (2.38-2.57)(7.7%) (2.22-2.37)(6.5%) (2.12-2.26)(6.4%) (1.98-2.13)(7.2%) (1.91-2.04)(6.6%)	57.81%	-22.72% -16.66% -30.3% -24.24% 16.66% -1.51% -3.03% 9.09%	50 x 50	2.4 GHZ WLAN Bluetooth 3.5 GHz WiMAX
[61]	Rectangular patch antenna connected to a tuning patch by a varactor (Simple)	3 Varactor	3.28	(2.6 - 4)(1% - 2.41%)	41.5%	141%	90 x 90	IoT
[111]	Compact loop antenna (Complex)	4 Varactors	0.9, 2.4, 3.5, 5.5	(0.698 - 0.96)(31.6%) (1.6 - 2.6)(47.6%) (3.4 - 3.8)(11.1%) (5 - 6)(18.1%)	143.75%	50.63% -64.87% -42.72%	25 x 10	2.4 GHz WLAN Bluetooth 5G WiFi 3.5 GHz WiMAX
[112]	Circular patch with reconfigurable shorting stubs (Complex)	9 Varactors	Triple bands: (2.51, 3.56, 4.62)	(2.22 - 2.79)(1%) (3.15 - 3.96)(1%) (4.23 - 5)(4% - 5.186%)	22.8%, 22.8% 16.7%	N/A, N/A 29.65%	131.47 x 131.47	IoT

WiFi, 4G WLAN and Bluetooth. The design in [15] provides the largest FBW of 28% for 5G WiFi applications, compared to the FBW reported in [109] (6.5%) and in [15] (10.16%). In terms of the 4G WLAN and Bluetooth applications, the largest FBW of 19.23% was achieved in [4] with a dual band reconfiguration. The FBW obtained in the same 4G WLAN spectrum in [15] is 16.66%. The reported work in [109] provided the largest TR for both single (86.42%) and dual bands tuning (57.5%, 20.5%), relative to [4] (35.29%) for single band and [4], [15] for dual band tuning of (21.27%, 14.88%) and (31.57%, 10.71%), respectively, as illustrated in Table 7. One highlight for utilizing PIN diodes for reconfiguring the 4G/5G spectrum into single, dual and triple bands would be the enhanced range of covered frequencies resulted from multi - band reconfiguration, which is observed in [4], [15], and [109].

Regarding the FBWC in the 4G/5G designs, the review of the reported works in [4], [15], and [109], which employed one, three and four PIN diodes respectively, reveals that employing a larger number of PIN diodes helps in increasing the FBW upon tuning. This is observed from the comparison of the FBWC values of reconfigured dual bands in [15] (45.5%, -10.08%) to the ones in [4] and [109] (21.27%, 14.88%) and (10.44%, 70.37%).

It is also observed that employing more PINs results in more band reconfigurations. However, this comes at a cost of increasing the footprint. This is highlighted when comparing the work in [109] of footprint ($27 \times 25\ mm^2$) which utilized

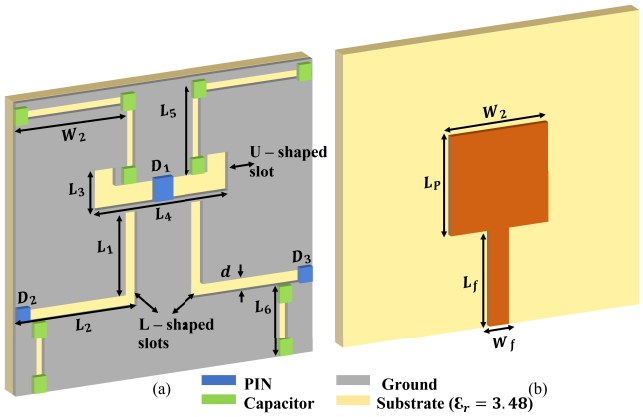

FIGURE 13. Antenna design for integrated 4G/5G frequency reconfigurability using PIN diodes (a) back view (b) front View. Adapted from [109].

three PINs to the work in [4] of footprint ($40 \times 32\ mm^2$), which emplyed four PINs.

The antennas presented in [19], [103], and [110] support similar applications using four, three and five PINs, respectively, including 2.4 GHz WLAN, Bluetooth and 3.5 GHz WiMAX. The structure in [103] offered an excellent Tuning Range (TR) of 76.13% compared to the TR values calculated from the data in [19] and [110] (27.28% and 57.81%, respectively.) For the 2.4 GHz WLAN band, the work presented in [19] offered a higher FBW of 12.24%, compared to the FBW in [103] and [110] which are 8.7% and 7.7%, respectively. However, for the 3.5 GHz WiMAX band, the work in [103] offered the largest FBW of 11.2%, compared to the FBW reported in [110] (5.5%) and in [19] (6.57%). Besides, the FBW demonstrated in [103] have generally improved upon tuning, with FBWC of 26.43% and 28.73%, for center frequencies 3.5 GHz and 5.35 GHz, respectively. However, a general FBW decrease was seen in [19] and [110] where the FBW deteriorated upon tuning to record an FBWC of-46.32% and -30.3%, respectively.

Varactors were also implemented for tuning purposes between 4G and 5G under similar bands [61], [111], [112]. The reported work in [111] have achieved the largest FBW for 2.4 GHz WLAN applications of 47.6%, with an incredible TR of 143.75%, which makes the design appropriate candidate for WLAN and Bluetooth, as well as for 5G WiFi and WiMAX applications. However, the FBW decreased upon tuning over the vast tuning range, with an FBWC of - 64.87%. On the other hand, the antennas presented in [61] and [112] have offered relatively narrow FBW, which is suitable for IoT applications. The design in [7] implemented three Varactors to achieve a FBW and TR values of of 2.41% and 41.5%, respectively, while the design in [112] used nine Varactors to offer a maximum TR of only 22.8 % and a maximum FBW of 5.18%. However, one merit for the design in [112] is the independently tunable triple band response, which irrespective of the narrow FBW in the first and second band (FBW = 1%) offers more coverage among the Sub-6 GHz spectrum.

In terms of the applications designated in the 4G and 5G bands (Sub-6 GHz), 4G application are included, where LTE 2300 was fully supported in [15], [103], [110], and [111]. The work in [4] has fully enabled LTE 2500, in addition to Bluetooth and WLAN that were covered in [4], [15], [19], [103], and [111]. Additional 5G services such as AMT (4.4 - 4.5) were supported in [109], 5G WLAN (5.725 - 5.825) in [4], [15], [109], and [111] and 3.5 GHz WiMAX (3.4 - 3.5) in [4], [15], [103], and [111]. The proposed antennas offer a great solution for the infrastructure required while taking a step into 5G but still need to support the established applications and standards.

The key observations on frequency reconfigurability in the intergrated 4G/5G spectrum are:

- Employing multiple PIN diodes improves obtained TR. This is noted when comparing the TR calculated in [15] to [109] and [103], as well as the TR in [110] to [4] and [19]. However, due to the discrete nature of the diode, a general decrease was observed when employing multiple PINs in the FBWC, as seen from comparing the FBWC calculated in [15], [109], and [103] to [19] and [110].
- Implementing multiple PIN diodes supports the reconfiguration of multiple bands (single, dual, triple). However, implementing multiple PIN diodes increases the footprint of the antenna [4], [109].

C. FREQUENCY RECONFIGURABILITY IN THE 5G SPECTRUM

Frequency tuning was also investigated in the 5G spectrum. The contemporary reported works found under in this spectrum were reviewed and compared [20], [113], [114], [115], [116] as demonstrated in Table 8. The design presented in [113] utilized four PINs to target 5G WLAN and 3.5 GHz WiMAX applications. The design achieved a TR of 44.44% but a decreasing FBW (FBWC = −40%), where the FBW offered for 5G WLAN band is 19.8%. The structures presented in [20] and [114] proposed tunable bands residing in the Sub-6GHz and utilized a combination of PINs and Varactors to support 5G WLAN applications. The design in [114] proposed an Ultra Wide Band (UWB) spanning from 3.19 to 5.47 GHz in addition to a tunable narrow band, while the work in [20] offered two bands, each can be tuned to three center frequencies, namely (3.21, 3.5, 3.63 GHz) and (4.76, 5.04, 5.42 GHz), respectively. The two bands together form an overlapping spectrum from 3.04 GHz to 5.89 GHz. When considering the works done in [20] and [114], the work in [20] achieved a higher TR of 51% compared to the TR of 44% achieved in [114]. On the other hand, a superior FBW improvement in [20] was calculated upon tuning from 15.3% to 39.7% (FBWC = 159.47%). Similarly, the FBW achieved in [114] improved upon tuning from 5% - 7.84%, where the FBWC calculated was 56.8%.

The significant FBW improvement calculated from [20] and [114] indicates the advantages of employing PINs and

TABLE 8. Comparison of the state of the art 5G frequency reconfigurable antennas.

	Figures of Merits							
Ref.	**Antenna Structure**	**No. of Switches**	**Fc (GHz)**	**S_{11} B.W. (GHz) (FBW %)**	**TR (%)**	**FBWC (%)**	**Footprint (mm^2)**	**Application**
[113]	Two dipoles fed through two coaxial cables and H - shaped slotted ground (Complex)	4 PIN	3.5, 5.5	(2.89 - 4.07) (33%) (5.1-6.19) (19.8%)	44.44%	-40%	50 x 50	5G WLAN 3.5 GHz WiMAX
[20]	Bow tie antenna (Complex)	2 Varactors, 2 PIN	Band 1: (3.21, 3.5, 3.63) Band 2: (4.76, 5.04, 5.42)	(3.04 - 5.89) (15.3% - 39.7%)	51%	159.47%	50 x 45	5G WLAN Cognitive Radio 5G WiFi
[114]	Wideband monpole and narrowband microstrip patch fed through a CPW structure (Complex)	3 Varactors, 2 PIN	4.33	UWB: (3.19 - 5.47) (52.65%) Narrowband: (3.4 - 5.32) (5% - 7.84%)	Narrowband: 44%	56.8%	75 x 35	5G WLAN 5G WiFi
[115]	Patch of merged half arc and right triangle (Simple)	2 PIN	Dual bands: (19.7,35.4) (20.5, 32.55) Triple bands: (17.2, 25.8, 35.75)	Dual bands: (17.85-21.81) (21.5%) (31.08 - 39.7) (24.32%) Triple bands: (18.47 - 22.51) (19.71%) (30.1 - 35) (14.92%) (16.38-18.04) (9.64%) (24.73 - 26.86) (8.25%) (32.95 - 38.55) (15.66%)	Dual bands: (4%, 8.38%)	Dual bands: (-8.32%, -38.65%)	7.5 x 5	Satellite Communication
[116]	Single layered patch antenna (Complex)	3 PIN	26.8, 28.01	(25.22 - 27.45) (8.32%) (26.41 - 28.89) (8.85%)	4.41%	6.37%	23.5 x 25.5	Satellite Communication

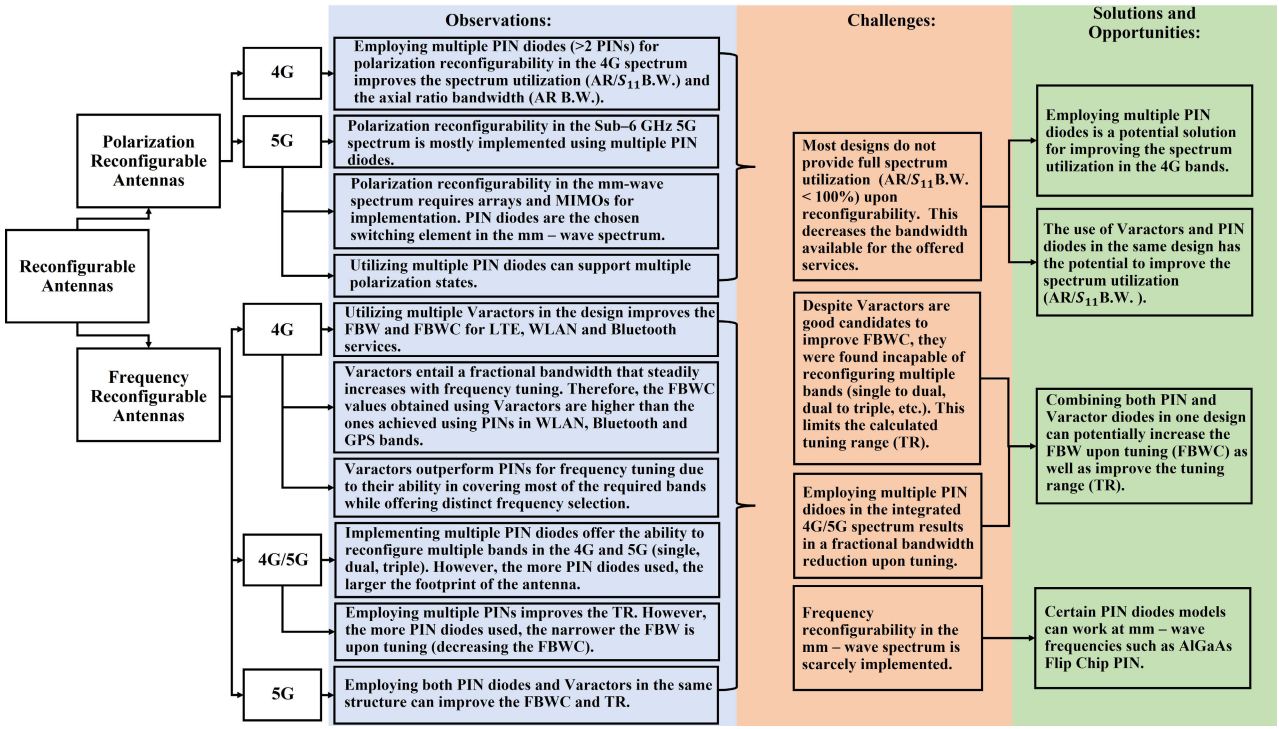

FIGURE 14. Observations, challenges and opportunities concluded from the review.

Varactors in the same structure. Varactors are able to tune the band locally, while the discrete nature of PIN diodes enables significant shift in the operating frequency or change its reconfiguration by manipulating the electrical length of the

antenna. Therefore, using PINs and Varactors for frequency tuning in the same antenna structure reaps the benefits of both diodes; employing multiple PINs enables multiple band reconfiguration, hence, a wider TR, while Varactors improve the FBW upon tuning, resulting in a significant FBWC. This is highlighted when comparing the designs in [20] and [114] to the work done in [113], which used four PIN diodes and obtained results inferior to [20] and [114].

The works done in [115] and [116] utilized PIN diodes for frequency tuning in the mm - wave 5G spectrum. The proposed works proved potentially useful for satellite communications. The design proposed in [115] utilized two AlGaAs Flip Chip PINs [117] and have achieved dual band reconfiguration (19.7, 35.4 GHz) to (20.5, 32.55 GHz) as well as triple bands centered around 17.2, 25.8, and 35.75 GHz, respectively. The design in [116] utilizes three PIN diodes and offers frequency shifting between center frequencies 26.8 GHz and 28.01 GHz, with a TR of 4.41 %. However, the offered FBW at 26.8 GHz and at 28.01 GHz, 8.32% and 8.85%, are very close to the ones reported in [115] (FBW = 8.25%) for the same band.

The key observations on frequency reconfiguration in the 5G spectrum are:

- Utilizing both PIN diodes and Varactors in the same antenna structure can improve the FBW upon tuning (FBWC) and TR in the Sub-6 GHz 5G spectrum, as seen from the works in [20], [113], and [114].
- The available implementations for frequency reconfigurable antennas in the mm - wave spectrum are scarce. This is due to the lack of commercially available switches that can support mm - wave frequencies. It is worth mentioning that Varactors can not be used at mm - wave frequencies due to their limited response time, which limits their performance at mm - wave frequencies [118], [119], [120].

V. OBSERVATIONS, CHALLENGES AND OPPORTUNITIES

Fig.14 highlights the main observations summarized as bullet points at the end of Subsection III-A and Subsection III-B for polarization reconfigurability and Subsection IV-A, Subsection IV-B and Subsection IV-C for frequency reconfigurability. The observations are concluded based on the change (increase / decrease) of the main figures of merits values, including, the newly defined spectrum utilization for polarization reconfigurability and the change in the fractional bandwdith for frequency reconfigruability, with respect to the type of electronic switch used (PINs / Varactors) as well as the number of these implemented switches. The challenges are also concluded based on the review of the concerned figures of merits for each type of reconfigurability. Solutions to the challenges and future opportunities for improvement are devised accordingly.

VI. CONCLUSION

A critical review of many modern 4G, 4G/5G and 5G implementations employing PIN diodes and Varactors for frequency or polarization reconfiguration was presented. The review of the reported works was done based on existing and newly defined figures of merits. For polarization diversity, the defined spectrum utilization, which is calculated based on the available axial ratio bandwidth and the impedance bandwidth was shown very useful in revealing the actual bandwidth available for the supported applications upon reconfiguration. Many modern designs failed to achieve full spectrum utilization, however it was observed that employing multiple PIN diodes for polarization diversity can improve the spectrum utilization and the axial ratio bandwdith in the 4G spectrum. For frequency reconfigurability, the comparison of the change in fractional bandwidth upon frequency tuning was shown essential in judging upon the performance of the reviewed reconfigured antennas in terms of the available fractional bandwdith for the supported applications upon tuning. It was observed that the employment of both PIN and Varactor diodes in one structure is very useful in improving the fractional bandwdith and tuning range in the 5G spectrum.

ACKNOWLEDGMENT

The authors would like to thank the University of Sharjah for the continued support and valuable resources.

REFERENCES

[1] C. Zhang, S. L. Ariyavisitakul, and M. Tao, "LTE-advanced and 4G wireless communications [guest editorial]," *IEEE Commun. Mag.*, vol. 50, no. 2, pp. 102–103, Feb. 2012.
[2] J.-H. Lu and J.-L. Guo, "Small-size octaband monopole antenna in an LTE/WWAN mobile phone," *IEEE Antennas Wireless Propag. Lett.*, vol. 13, pp. 548–551, 2014.
[3] N. O. Parchin, H. J. Basherlou, Y. I. A. Al-Yasir, A. M. Abdulkhaleq, and R. A. Abd-Alhameed, "Reconfigurable antennas: Switching techniques—A survey," *Electronics*, vol. 9, no. 2, p. 336, Feb. 2020.
[4] H. Dildar, F. Althobiani, I. Ahmad, W. U. R. Khan, S. Ullah, N. Mufti, S. Ullah, F. Muhammad, M. Irfan, and A. Glowacz, "Design and experimental analysis of multiband frequency reconfigurable antenna for 5G and Sub-6 GHz wireless communication," *Micromachines*, vol. 12, no. 1, p. 32, Dec. 2020.
[5] W. Pan, C. Huang, P. Chen, M. Pu, X. Ma, and X. Luo, "A beam steering horn antenna using active frequency selective surface," *IEEE Trans. Antennas Propag.*, vol. 61, no. 12, pp. 6218–6223, Dec. 2013.
[6] M. W. Young, S. Yong, and J. T. Bernhard, "A miniaturized frequency reconfigurable antenna with single bias, dual varactor tuning," *IEEE Trans. Antennas Propag.*, vol. 63, no. 3, pp. 946–951, Mar. 2015.
[7] N. Nguyen-Trong, A. Piotrowski, and C. Fumeaux, "A frequency-reconfigurable dual-band low-profile monopolar antenna," *IEEE Trans. Antennas Propag.*, vol. 65, no. 7, pp. 3336–3343, Jul. 2017.
[8] S. Gao, A. Sambell, and S. S. Zhong, "Polarization-agile antennas," *IEEE Antennas Propag. Mag.*, vol. 48, no. 3, pp. 28–37, Jun. 2006.
[9] L. Kang, H. Li, J. Zhou, and S. Zheng, "An OAM-mode reconfigurable array antenna with polarization agility," *IEEE Access*, vol. 8, pp. 40445–40452, 2020.
[10] M. N. Osman, M. K. A. Rahim, M. R. Hamid, M. F. M. Yusoff, and H. A. Majid, "Compact dual-port polarization-reconfigurable antenna with high isolations for MIMO application," *IEEE Antennas Wireless Propag. Lett.*, vol. 15, pp. 456–459, 2016.
[11] C. G. Christodoulou, Y. Tawk, S. A. Lane, and S. R. Erwin, "Reconfigurable antennas for wireless and space applications," *Proc. IEEE*, vol. 100, no. 7, pp. 2250–2261, Jul. 2012.
[12] I. Ahmad, H. Dildar, W. U. R. Khan, S. A. A. Shah, S. Ullah, S. Ullah, S. M. Umar, M. A. Albreem, M. H. Alsharif, and K. Vasudevan, "Design and experimental analysis of multiband compound reconfigurable 5G antenna for sub-6 GHz wireless applications," *Wireless Commun. Mobile Comput.*, vol. 2021, pp. 1–14, Apr. 2021.

[13] R. L. Haupt and M. Lanagan, "Reconfigurable antennas," *IEEE Antennas Propag. Mag.*, vol. 55, no. 1, pp. 49–61, Feb. 2013.

[14] N. O. Parchin, H. J. Basherlou, Y. I. Al-Yasir, R. A. Abd-Alhameed, A. M. Abdulkhaleq, and J. M. Noras, "Recent developments of reconfigurable antennas for current and future wireless communication systems," *Electronics*, vol. 8, no. 2, p. 128, 2019.

[15] R. Shanmugam, "Design and analysis of a frequency reconfigurable penta-band antenna for WLAN and 5G applications," *J. Electromagn. Eng. Sci.*, vol. 21, no. 3, pp. 228–235, Jul. 2021.

[16] F. Zadehparizi and S. Jam, "Increasing reliability of frequency-reconfigurable antennas," *IEEE Antennas Wireless Propag. Lett.*, vol. 17, no. 5, pp. 920–923, May 2018.

[17] M. M. Fakharian, P. Pezaei, A. A. Orouji, and M. Soltanpur, "A wide-band and reconfigurable filtering slot antenna," *IEEE Antennas Wireless Propag. Lett.*, vol. 15, pp. 1610–1613, 2016.

[18] L. Pazin and Y. Leviatan, "Reconfigurable slot antenna for switchable multiband operation in a wide frequency range," *IEEE Antennas Wireless Propag. Lett.*, vol. 12, pp. 329–332, 2013.

[19] G. Jin, C. Deng, J. Yang, Y. Xu, and S. Liao, "A new differentially-fed frequency reconfigurable antenna for WLAN and sub-6GHz 5G applications," *IEEE Access*, vol. 7, pp. 56539–56546, 2019.

[20] T. Li, H. Zhai, L. Li, and C. Liang, "Frequency-reconfigurable bow-tie antenna with a wide tuning range," *IEEE Antennas Wireless Propag. Lett.*, vol. 13, pp. 1549–1552, 2014.

[21] Z. Zhang and Z. Pan, "Design of reconfigurable bandwidth filtering antenna and its applications in IR/UWB system," *Electronics*, vol. 9, no. 1, p. 163, Jan. 2020.

[22] P. F. Hu, Y. M. Pan, X. Y. Zhang, and B.-J. Hu, "A filtering patch antenna with reconfigurable frequency and bandwidth using F-shaped probe," *IEEE Trans. Antennas Propag.*, vol. 67, no. 1, pp. 121–130, Jan. 2019.

[23] N. Ojaroudi, S. Amiri, and F. Geran, "A novel design of reconfigurable monopole antenna for UWB applications," *Appl. Comput. Electromagn. Soc. J.*, vol. 28, no. 7, pp. 633–639, 2013.

[24] J. Deng, S. Hou, L. Zhao, and L. Guo, "Wideband-to-narrowband tunable monopole antenna with integrated bandpass filters for UWB/WLAN applications," *IEEE Antennas Wireless Propag. Lett.*, vol. 16, pp. 2734–2737, 2017.

[25] P. Y. Qin, F. Wei, and Y. J. Guo, "A wideband-to-narrowband tunable antenna using a reconfigurable filter," *IEEE Trans. Antennas Propag.*, vol. 63, no. 5, pp. 2282–2285, May 2014.

[26] M.-C. Tang, Z. Wen, H. Wang, M. Li, and R. W. Ziolkowski, "Compact, frequency-reconfigurable filtenna with sharply defined wideband and continuously tunable narrowband states," *IEEE Trans. Antennas Propag.*, vol. 65, no. 10, pp. 5026–5034, Oct. 2017.

[27] I. F. Da Costa, S. A. Cerqueira, D. H. Spadoti, L. G. Da Silva, J. A. J. Ribeiro, and S. E. Barbin, "Optically controlled reconfigurable antenna array for mm-Wave applications," *IEEE Antennas Wireless Propag. Lett.*, vol. 16, pp. 2142–2145, 2017.

[28] P. Alizadeh, A. S. Andy, C. Parini, and K. Z. Rajab, "A reconfigurable reflectarray antenna in Ka-band using optically excited silicon," in *Proc. 10th Eur. Conf. Antennas Propag. (EuCAP)*, Apr. 2016, pp. 1–5.

[29] P.-J. Liu, D.-S. Zhao, and B.-Z. Wang, "Design of optically controlled microwave switch for reconfigurable antenna systems," in *Proc. Int. Conf. Microw. Millim. Wave Technol.*, vol. 1, Apr. 2007, Art. no. 90505001.

[30] Y. Tawk, J. Costantine, F. Ayoub, C. Christodoulou, D. Doyle, and S. A. Lane, "Physically reconfigurable antennas: Concepts and automation," in *Proc. IEEE Int. Symp. Antennas Propag. USNC/URSI Nat. Radio Sci. Meeting*, Jul. 2017, pp. 419–420.

[31] I. T. McMichael, "A mechanically reconfigurable patch antenna with polarization diversity," *IEEE Antennas Wireless Propag. Lett.*, vol. 17, no. 7, pp. 1186–1189, Jul. 2018.

[32] J. Costantine, Y. Tawk, S. E. Barbin, and C. G. Christodoulou, "Reconfigurable antennas: Design and applications," *Proc. IEEE*, vol. 103, no. 3, pp. 424–437, Mar. 2015.

[33] P. Liu, S. Yang, X. Wang, M. Yang, J. Song, and L. Dong, "Directivity-reconfigurable wideband two-arm spiral antenna," *IEEE Antennas Wireless Propag. Lett.*, vol. 16, pp. 66–69, 2016.

[34] Z. Hu, S. Wang, Z. Shen, and W. Wu, "Broadband polarization-reconfigurable water spiral antenna of low profile," *IEEE Antennas Wireless Propag. Lett.*, vol. 16, pp. 1377–1380, 2017.

[35] S. Wang, L. Zhu, and W. Wu, "A novel frequency-reconfigurable patch antenna using low-loss transformer oil," *IEEE Trans. Antennas Propag.*, vol. 65, no. 12, pp. 7316–7321, Dec. 2017.

[36] S. J. Mazlouman, A. Mahanfar, C. Menon, and R. G. Vaughan, "A review of mechanically reconfigurable antennas using smart material actuators," in *Proc. 5th Eur. Conf. Antennas Propag. (EUCAP)*, Apr. 2011, pp. 1076–1079.

[37] T. N. Ibrahim, T. Harvey, B. Dane, P. L. Craig, and M. W. Thomas, "Mechanically reconfigurable, dual-band slot dipole antennas," *IEEE Trans. Antennas Propag.*, vol. 63, no. 7, pp. 3267–3271, Jul. 2015.

[38] P. Sanchez-Olivares and J. L. Masa-Campos, "Mechanically reconfigurable conformal array antenna fed by radial waveguide divider with tuning screws," *IEEE Trans. Antennas Propag.*, vol. 65, no. 9, pp. 4886–4890, Sep. 2017.

[39] T. S. Teeslink, D. Torres, J. L. Ebel, N. Sepulveda, and D. E. Anagnostou, "Reconfigurable bowtie antenna using metal-insulator transition in vanadium dioxide," *IEEE Antennas Wireless Propag. Lett.*, vol. 14, pp. 1381–1384, 2015.

[40] M. Wang, I. M. Kilgore, M. B. Steer, and J. J. Adams, "Characterization of intermodulation distortion in reconfigurable liquid metal antennas," *IEEE Antennas Wireless Propag. Lett.*, vol. 17, no. 2, pp. 279–282, Feb. 2018.

[41] G. B. Zhang, R. C. Gough, M. R. Moorefield, K. J. Cho, A. T. Ohta, and W. A. Shiroma, "A liquid-metal polarization-pattern-reconfigurable dipole antenna," *IEEE Antennas Wireless Propag. Lett.*, vol. 17, pp. 50–53, 2018.

[42] I. F. Akyildiz, D. M. Gutierrez-Estevez, and E. C. Reyes, "The evolution to 4G cellular systems: LTE-advanced," *Phys. Commun.*, vol. 3, no. 4, pp. 217–244, 2010. [Online]. Available: https://www.sciencedirect.com/science/article/pii/S1874490710000303

[43] F. Firmin. (2015). *3GPP Portal*. [Online]. Available: https://portal.3gpp.org/desktopmodules/Specifications/SpecificationDetails.aspx?specificationId=1072

[44] S. Frattasi, H. Fathi, F. H. P. Fitzek, R. Prasad, and M. D. Katz, "Defining 4G technology from the users perspective," *IEEE Netw.*, vol. 20, no. 1, pp. 35–41, Jan. 2006.

[45] R. S. H. Istepanaian and Y.-T. Zhang, "Guest editorial introduction to the special section: 4G health—The long-term evolution of m-health," *IEEE Trans. Inf. Technol. Biomed.*, vol. 16, no. 1, pp. 1–5, Jan. 2012.

[46] P. P. Parikh, M. G. Kanabar, and T. S. Sidhu, "Opportunities and challenges of wireless communication technologies for smart grid applications," in *Proc. IEEE PES Gen. Meeting*, Jul. 2010, pp. 1–7.

[47] M. Y. Rhee, "4G wireless internet communication technology," in *Wireless Mobile Internet Security*. Wiley, 2013, pp. 439–465, doi: 10.1002/9781118512920.ch13.

[48] H. T. Chattha, "4-port 2-element MIMO antenna for 5G portable applications," *IEEE Access*, vol. 7, pp. 96516–96520, 2019.

[49] Q. Wu, P. Liang, and X. Chen, "A broadband ±45° dual-polarized multiple-input multiple-output antenna for 5G base stations with extra decoupling elements," *J. Commun. Inf. Netw.*, vol. 3, no. 1, pp. 31–37, Mar. 2018.

[50] (Jun. 2022). *5G Spectrum—GSMA*. [Online]. Available: https://www.gsma.com/spectrum/wp-content/uploads/2022/06/5G-Spectrum-Positions.pdf

[51] M. Khalily, R. Tafazolli, P. Xiao, and A. A. Kishk, "Broadband mm-Wave Microstrip array antenna with improved radiation characteristics for different 5G applications," *IEEE Trans. Antennas Propag.*, vol. 66, no. 9, pp. 4641–4647, Sep. 2018.

[52] S. Kumar, A. S. Dixit, R. R. Malekar, H. D. Raut, and L. K. Shevada, "Fifth generation antennas: A comprehensive review of design and performance enhancement techniques," *IEEE Access*, vol. 8, pp. 163568–163593, 2020.

[53] *Requirements, Evaluation Criteria and Submission Templates for the Development of IMT-2020*, document M.2411, Nov. 2017.

[54] X. Lu, E. Sopin, V. Petrov, O. Galinina, D. Moltchanov, K. Ageev, S. Andreev, Y. Koucheryavy, K. Samouylov, and M. Dohler, "Integrated use of licensed- and unlicensed-band mmWave radio technology in 5G and beyond," *IEEE Access*, vol. 7, pp. 24376–24391, 2019.

[55] H. Hui, Y. Ding, Q. Shi, F. Li, Y. Song, and J. Yan, "5G network-based Internet of Things for demand response in smart grid: A survey on application potential," *Appl. Energy*, vol. 257, Jan. 2020, Art. no. 113972. [Online]. Available: https://www.sciencedirect.com/science/article/pii/S0306261919316599

[56] *IMT Vision–Framework and Overall Objectives of the Future Development of IMT for 2020 and Beyond*, document TU-R M.2083-0, 2015.

[57] M. Ikram, E. A. Abbas, N. Nguyen-Trong, K. H. Sayidmarie, and A. Abbosh, "Integrated frequency-reconfigurable slot antenna and connected slot antenna array for 4G and 5G mobile handsets," *IEEE Trans. Antennas Propag.*, vol. 67, no. 12, pp. 7225–7233, Dec. 2019.

[58] A. Khidre, F. Yang, and A. Z. Elsherbeni, "A patch antenna with a varactor-loaded slot for reconfigurable dual-band operation," *IEEE Trans. Antennas Propag.*, vol. 63, no. 2, pp. 755–760, Feb. 2015.
[59] C. Huang, W. Pan, X. Ma, and X. Luo, "A frequency reconfigurable directive antenna with wideband low-RCS property," *IEEE Trans. Antennas Propag.*, vol. 64, no. 3, pp. 1173–1178, Mar. 2016.
[60] L. Ge, M. Li, J. Wang, and H. Gu, "Unidirectional dual-band stacked patch antenna with independent frequency reconfiguration," *IEEE Antennas Wireless Propag. Lett.*, vol. 16, pp. 113–116, 2016.
[61] N. Nguyen-Trong and C. Fumeaux, "Tuning range and efficiency optimization of a frequency-reconfigurable patch antenna," *IEEE Antennas Wireless Propag. Lett.*, vol. 17, no. 1, pp. 150–154, Jan. 2018.
[62] Skyworks. (Oct. 23, 2022). *Application Note Varactor Diode*. [Online]. Available: https://www.skyworksinc.com/-/media/900F2141E45048DAA0A60CD40E8F567B.pdf
[63] (Apr. 2020). *Data Sheet SMV2019 to SMV2023 Series: Hyperabrupt Junction…Skyworks*. [Online]. Available: https://www.skyworksinc.com/-/media/SkyWorks/Documents/Products/201-300/SMV2019_to_SMV2023_Series_200074S.pdf
[64] A. Singh, K. Shet, D. Prasat, A. K. Pandey, and M. Aneesh, "A review: Circuit theory of microstrip antennas for dual-, multi-, and ultra-widebands," in *Modulation in Electronics and Telecommunications*, G. Dekoulis, Ed. London, U.K.: IntechOpen, 2020, pp. 105–123.
[65] S. Verma and J. A. Ansari, "Analysis of U-slot loaded truncated corner rectangular microstrip patch antenna for broadband operation," *AEU Int. J. Electron. Commun.*, vol. 69, no. 10, pp. 1483–1488, Oct. 2015.
[66] Y. Zhang, Q. Yin, M. Luo, and Y. Jiang, "The pin diode circuit designers, handbook the pin diode circuit designers, handbook, 1998," *IEICE Trans. Commun.*, vol. 90, no. 6, pp. 1467–1473, 2007.
[67] R. Cory and D. Fryklund, "Solid state RF/microwave switch technology: Part 2," in *Microw. Product Dig.*, 2009, p. 34.
[68] S. Dubal and A. Chaudhari, "Mechanisms of reconfigurable antenna: A review," in *Proc. 10th Int. Conf. Cloud Comput., Data Sci. Eng. (Confluence)*, Jan. 2020, pp. 576–580.
[69] X. Li, F. Xiao, Y. Luo, R. Wang, and Y. Duan, "Modeling of high-voltage nonpunch-through PIN diode snappy reverse recovery and its optimal suppression method based on RC snubber circuit," *IEEE Trans. Ind. Electron.*, vol. 69, no. 6, pp. 5700–5712, Jun. 2022.
[70] K. Shenai, M. Trivedi, and P. G. Neudeck, "Characterization of hard- and soft-switching performance of high-voltage Si and 4H-SiC PiN diodes," *IEEE Trans. Electron Devices*, vol. 49, no. 9, pp. 1648–1656, Sep. 2002.
[71] S. W. Lee and Y. J. Sung, "Reconfigurable rhombus-shaped patch antenna with Y-shaped feed for polarization diversity," *IEEE Antennas Wireless Propag. Lett.*, vol. 14, pp. 163–166, 2015.
[72] *Hsmp-3860 Datasheet, Equivalent, Pin Diodes*. Accessed: Oct. 2022. [Online]. Available: https://datasheetspdf.com/pdf/860530/AVAGO/HSMP-3860/1
[73] *C St Studio Suite 2013*, Computer Simulation Technology AG, Darmstadt, Germany, 2013.
[74] S. K. Patel, S. P. Lavadiya, J. Parmar, K. Ahmed, S. A. Taya, and S. Das, "Low-cost, multiband, high gain and reconfigurable microstrip radiating structure using PIN diode for 5G/Wi-MAX/WLAN applications," *Phys. B, Condens. Matter*, vol. 639, Aug. 2022, Art. no. 413972.
[75] W. A. Awan, N. Hussain, S. Kim, and N. Kim, "A frequency-reconfigurable filtenna for GSM, 4G-LTE, ISM, and 5G Sub-6 GHz band applications," *Sensors*, vol. 22, no. 15, p. 5558, Jul. 2022.
[76] D. Schaubert, F. Farrar, A. Sindoris, and S. Hayes, "Microstrip antennas with frequency agility and polarization diversity," *IEEE Trans. Antennas Propag.*, vol. AP-29, no. 1, pp. 118–123, Jan. 1981.
[77] S.-G. Zhou, G.-L. Huang, H.-Y. Liu, A.-S. Lin, and C.-Y.-D. Sim, "A CPW-fed square-ring slot antenna with reconfigurable polarization," *IEEE Access*, vol. 6, pp. 16474–16483, 2018.
[78] W. Lin and H. Wong, "Polarization reconfigurable wheel-shaped antenna with conical-beam radiation pattern," *IEEE Trans. Antennas Propag.*, vol. 63, no. 2, pp. 491–499, Feb. 2015.
[79] W. Lin and H. Wong, "Wideband circular-polarization reconfigurable antenna with L-shaped feeding probes," *IEEE Antennas Wireless Propag. Lett.*, vol. 16, pp. 2114–2117, 2017.
[80] K. X. Wang and H. Wong, "A reconfigurable CP/LP antenna with cross-probe feed," *IEEE Antennas Wireless Propag. Lett.*, vol. 16, pp. 669–672, 2017.
[81] E. Al Abbas, N. Nguyen-Trong, A. T. Mobashsher, and A. M. Abbosh, "Polarization-reconfigurable antenna array for millimeter-wave 5G," *IEEE Access*, vol. 7, pp. 131214–131220, 2019.
[82] J.-S. Row and M.-J. Hou, "Design of polarization diversity patch antenna based on a compact reconfigurable feeding network," *IEEE Trans. Antennas Propag.*, vol. 62, no. 10, pp. 5349–5352, Oct. 2014.
[83] J. Hu, Z. C. Hao, and Z. W. Miao, "Design and implementation of a planar polarization-reconfigurable antenna," *IEEE Antennas Wireless Propag. Lett.*, vol. 16, pp. 1557–1560, 2017.
[84] M. Li, Z. Zhang, and M.-C. Tang, "A compact, low-profile, wideband, electrically controlled, tri-polarization-reconfigurable antenna with quadruple gap-coupled patches," *IEEE Trans. Antennas Propag.*, vol. 68, no. 8, pp. 6395–6400, Aug. 2020.
[85] L. Ge, X. Yang, M. Li, and H. Wong, "Polarization-reconfigurable magnetoelectric dipole antenna for 5G Wi-Fi," *IEEE Antennas Wireless Propag. Lett.*, vol. 16, pp. 1504–1507, 2017.
[86] S. W. Lee and Y. J. Sung, "Simple polarization-reconfigurable antenna with T-shaped feed," *IEEE Antennas Wireless Propag. Lett.*, vol. 15, pp. 114–117, 2016.
[87] J.-S. Row, W.-L. Liu, and T.-R. Chen, "Circular polarization and polarization reconfigurable designs for annular slot antennas," *IEEE Trans. Antennas Propag.*, vol. 60, no. 12, pp. 5998–6002, Dec. 2012.
[88] M. Ali, *Reconfigurable Antenna Design and Analysis*. Norwood, MA, USA: Artech House, 2021.
[89] J. S. Seybold, *Introduction to RF propagation*. Hoboken, NJ, USA: Wiley, 2005.
[90] A. Khidre, K.-F. Lee, F. Yang, and A. Z. Elsherbeni, "Circular polarization reconfigurable wideband E-shaped patch antenna for wireless applications," *IEEE Trans. Antennas Propag.*, vol. 61, no. 2, pp. 960–964, Feb. 2013.
[91] A. Panahi, X. L. Bao, K. Yang, O. O'Conchubhair, and M. J. Ammann, "A simple polarization reconfigurable printed monopole antenna," *IEEE Trans. Antennas Propag.*, vol. 63, no. 11, pp. 5129–5134, Nov. 2015.
[92] C.-Y.-D. Sim, Y.-J. Liao, and H.-L. Lin, "Polarization reconfigurable eccentric annular ring slot antenna design," *IEEE Trans. Antennas Propag.*, vol. 63, no. 9, pp. 4152–4155, Sep. 2015.
[93] X.-X. Yang, B.-C. Shao, F. Yang, A. Z. Elsherbeni, and B. Gong, "A polarization reconfigurable patch antenna with loop slots on the ground plane," *IEEE Antennas Wireless Propag. Lett.*, vol. 11, pp. 69–72, 2012.
[94] W. Lin and H. Wong, "Wideband circular polarization reconfigurable antenna," *IEEE Trans. Antenna Propag.*, vol. 63, no. 12, pp. 5938–5944, Dec. 2015.
[95] J. F. Tsai and J. S. Row, "Reconfigurable square-ring microstrip antenna," *IEEE Trans. Antennas Propag.*, vol. 61, no. 5, pp. 2857–2860, May 2013.
[96] (Mar. 2014). *1559-1610 MHz*. [Online]. Available: Mhttps://www.ntia.doc.gov/files/ntia/publications/compendium/1559.00-1610.00_01MAR14.pdf
[97] Y. I. Al-Yasir, A. S. Abdullah, N. O. Parchin, R. A. Abd-Alhameed, and J. M. Noras, "A new polarization-reconfigurable antenna for 5G applications," *Electronics*, vol. 7, no. 11, p. 293, 2018.
[98] Z. Wu, H. Liu, and L. Li, "Metasurface-inspired low profile polarization reconfigurable antenna with simple DC controlling circuit," *IEEE Access*, vol. 7, pp. 45073–45079, 2019.
[99] F. Ferrero, C. Luxey, R. Staraj, G. Jacquemod, M. Yedlin, and V. Fusco, "A novel quad-polarization agile patch antenna," *IEEE Trans. Antennas Propag.*, vol. 57, no. 5, pp. 1563–1567, May 2009.
[100] S. Kim and J. Kim, "Design of reconfigurable antenna feeding network using coupled-line switch for 5G millimeter-wave communication system," *Appl. Comput. Electromagn. Soc. J.*, VOL. 33, NO. 8, pp. 861–867, 2018.
[101] A. T. Alreshaid, Y. Cui, R. Bahr, M. M. Tentzeris, and M. S. Sharawi, "A millimeter wave tri-polarized patch antenna with a bandwidth-enhancing parasitic element," in *Proc. IEEE Int. Symp. Antennas Propag. USNC-URSI Radio Sci. Meeting (APS/URSI)*, Dec. 2021, pp. 1051–1052.
[102] N. Sultan, W. F. T. Payne, R. R. Musclow, and M. Bouchard, "Reconfigurable dual feed antenna for direct broadcast satellites," *Acta Astronautica*, vol. 12, no. 1, pp. 27–35, Jan. 1985.
[103] M. Borhani, P. Rezaei, and A. Valizade, "Design of a reconfigurable miniaturized microstrip antenna for switchable multiband systems," *IEEE Antennas Wireless Propag. Lett.*, vol. 15, pp. 822–825, 2016.
[104] S. Yang, Y. Chen, C. Yu, Y. Gong, and F. Tong, "Design of a low-profile, frequency-reconfigurable, and high gain antenna using a varactor-loaded AMC ground," *IEEE Access*, vol. 8, pp. 158635–158646, 2020.
[105] S. Danesh, S. K. A. Rahim, M. Abedian, and M. R. Hamid, "A compact frequency-reconfigurable dielectric resonator antenna for LTE/WWAN and WLAN applications," *IEEE Antennas Wireless Propag. Lett.*, vol. 14, pp. 486–489, 2015.

[106] R. Hussain, M. U. Khan, N. Iqbal, E. AlMajali, S. S. Alja'Afreh, U. Johar, A. Shamim, and M. S. Sharawi, "Frequency agile multiple-input-multiple-output antenna design for 5G dynamic spectrum sharing in cognitive radio networks," *Microw. Opt. Technol. Lett.*, vol. 63, no. 3, pp. 889–894, Mar. 2021.
[107] J.-S. Row and J.-F. Tsai, "Frequency-reconfigurable microstrip patch antennas with circular polarization," *IEEE Antennas Wireless Propag. Lett.*, vol. 13, pp. 1112–1115, 2014.
[108] M. Mani, R. Moolat, S. V. Abdulrahiman, A. P. Viswanathan, V. Kesavath, and M. Pezholil, "Frequency reconfigurable stepped impedance dipole antenna for wireless applications," *AEU Int. J. Electron. Commun.*, vol. 115, Feb. 2020, Art. no. 153029.
[109] L. Han, C. Wang, X. Chen, and W. Zhang, "Compact frequency-reconfigurable slot antenna for wireless applications," *IEEE Antennas Wireless Propag. Lett.*, vol. 15, pp. 1795–1798, 2016.
[110] H. A. Majid, M. K. A. Rahim, M. R. Hamid, N. A. Murad, and M. F. Ismail, "Frequency-reconfigurable microstrip patch-slot antenna," *IEEE Antennas Wireless Propag. Lett.*, vol. 12, pp. 218–220, 2013.
[111] S. Subbaraj, M. Kanagasabai, M. G. N. Alsath, S. K. Palaniswamy, S. Kingsly, I. Kulandhaisamy, A. K. Shrivastav, R. Natarajan, and S. Meiyalagan, "A compact frequency-reconfigurable antenna with independent tuning for hand-held wireless devices," *IEEE Trans. Antennas Propag.*, vol. 68, no. 2, pp. 1151–1154, Feb. 2020.
[112] K. Paramayudha, S. Jammy Chen, T. Kaufmann, W. Withayachumnankul, and C. Fumeaux, "Triple-band reconfigurable low-profile monopolar antenna with independent tunability," *IEEE Open J. Antennas Propag.*, vol. 1, pp. 47–56, 2020.
[113] G. Jin, C. Deng, Y. Xu, J. Yang, and S. Liao, "Differential frequency-reconfigurable antenna based on dipoles for sub-6 GHz 5G and WLAN applications," *IEEE Antennas Wireless Propag. Lett.*, vol. 19, no. 3, pp. 472–476, Mar. 2020.
[114] T. K. Nguyen, C. D. Bui, A. Narbudowicz, and N. Nguyen-Trong, "Frequency-reconfigurable antenna with wide- and narrowband modes for sub-6 GHz cognitive radio," *IEEE Antennas Wireless Propag. Lett.*, vol. 22, no. 1, pp. 64–68, Jan. 2023.
[115] W. A. Awan, N. Hussain, A. Ghaffar, S. Naqvi, A. Zaidi, M. Hussain, and X. J. Li, "A low profile frequency reconfigurable antenna for mmWave applications," in *WITS 2020*. Cham, Switzerland: Springer, 2022, pp. 1073–1083.
[116] M. K. Shereen and M. I. Khattak, "A hybrid reconfigurability structure and improved gain characteristics for a novel 5G monopole antenna for future mobile communication," *Wireless Pers. Commun.*, vol. 123, no. 2, pp. 1841–1853, Mar. 2022.
[117] Macom. *Algaas Flip-Chip Pin Diode 100 MHz to 50 GHz*. Accessed: Dec. 2023. [Online]. Available: https://www.te.com/commerce/DocumentDelivery/DDEController
[118] *Silicon Abrupt Tuning Varactor Diodes*. Accessed: Nov. 2022. [Online]. Available: https://datasheetspdf.com/pdf-file/1299220/MACOM/SMV1401/1
[119] *Surface Mount Tuning Varactors Series*. Accessed: Nov. 2022. [Online]. Available: https://www.digchip.com/datasheets/download_datasheet.php?id=888477&part-number=SMTD3001
[120] C. Poole and I. Darwazeh, "Microwave semiconductor materials and diodes," in *Microwave Active Circuit Analysis and Design*, C. Poole and I. Darwazeh, Eds. Oxford, u.k.: Academic, 2016, ch. 11, pp. 355–393. [Online]. Available: https://www.sciencedirect.com/science/article/pii/B9780124078239000111

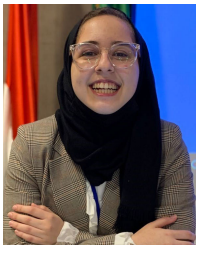

RAZAN ALHAMAD (Student Member, IEEE) was born in Fujairah, United Arab Emirates, in 1999. She received the B.Sc. degree in communications engineering from Aldar University College, Dubai, United Arab Emirates, in 2016. She is currently pursuing the M.Sc. degree in electrical and electronics engineering with the Electrical Engineering Department, University of Sharjah, Sharjah, United Arab Emirates. She has been a Graduate Research Assistant with the Mixed Analog–Digital Smart Electronics Circuit and Systems (MADSECS) Research Group, University of Sharjah, since 2020.

EQAB ALMAJALI (Member, IEEE) received the B.Sc. degree (Hons.) from Mu'tah University, Jordan, and the M.A.Sc. and Ph.D. degrees (Hons.) in electrical engineering from the University of Ottawa, Ottawa, ON, Canada, in 2010 and 2014, respectively.

He has been an Assistant Professor with the Electrical Engineering Department, University of Sharjah, since August 2017. Prior to that, he was a Postdoctoral Fellow with the Electronics Department, Carleton University, Canada. He is the author of more than 50 technical publications and two book chapters. His current research interests include frequency selective surfaces, millimeter-wave MIMO antennas, reconfigurable antennas, RF passive and active sensors, THz antennas, and wireless power transfer. He received the prestigious Canadian National Science and Engineering Research Council (NSERC) Postdoctoral Fellowship for his research excellence, in 2014, and also received the NSERC-PGS Scholarship during his doctoral studies, in 2012.

SOLIMAN MAHMOUD (Senior Member, IEEE) was born in Cairo, Egypt, in 1971. He received the B.Sc. (Hons.), M.Sc., and Ph.D. degrees from the Electronics and Communications Department, Cairo University, Egypt, in 1994, 1996, and 1999, respectively.

He is currently a Professor and the Department Chairperson with the Electrical Engineering Department, University of Sharjah, Sharjah, United Arab Emirates. He supervised two Ph.D. students, 14 M.Sc. students, and more than 40 senior design projects. He is actively engaged in scholarly research work and has authored or coauthored more than 170 journals and conference publications since joining academia, in 1996. He received "The German-Egyptian Research Fund" Grant. The Grant has been used to finance the project "Design of CMOS Field Programmable Analog Array and Its Applications." The project has been carried out in collaboration with the Ulm Microelectronics Institute, Ulm University, Germany. His articles received more than 2100 citations and his Google Scholar H-index is 25 (H-index from Scopus is 22). He published six refereed research books. His research interests include mixed analog/digital integrated electronic circuit (IC) design, including mixed mode (voltage/current) analog circuits IC design, mixed (analog/digital) programmable CMOS electronics systems, biomedical circuits, field programmable analog arrays (FPAAs), and multi-standard wireless receiver design. In 2005, he received the Science Prize in Advanced Engineering Technology from the Academy of Scientific Research and Technology, Higher Ministry of Education, Cairo. He received the Distinguished Research Award from the University of Sharjah, from 2011 to 2012 and from 2014 to 2015.